

THE SUNRISE III MISSION & DKIST

ANDREAS LAGG
MPI FOR SOLAR SYSTEM RESEARCH, GÖTTINGEN



JOHNS HOPKINS
APPLIED PHYSICS LABORATORY



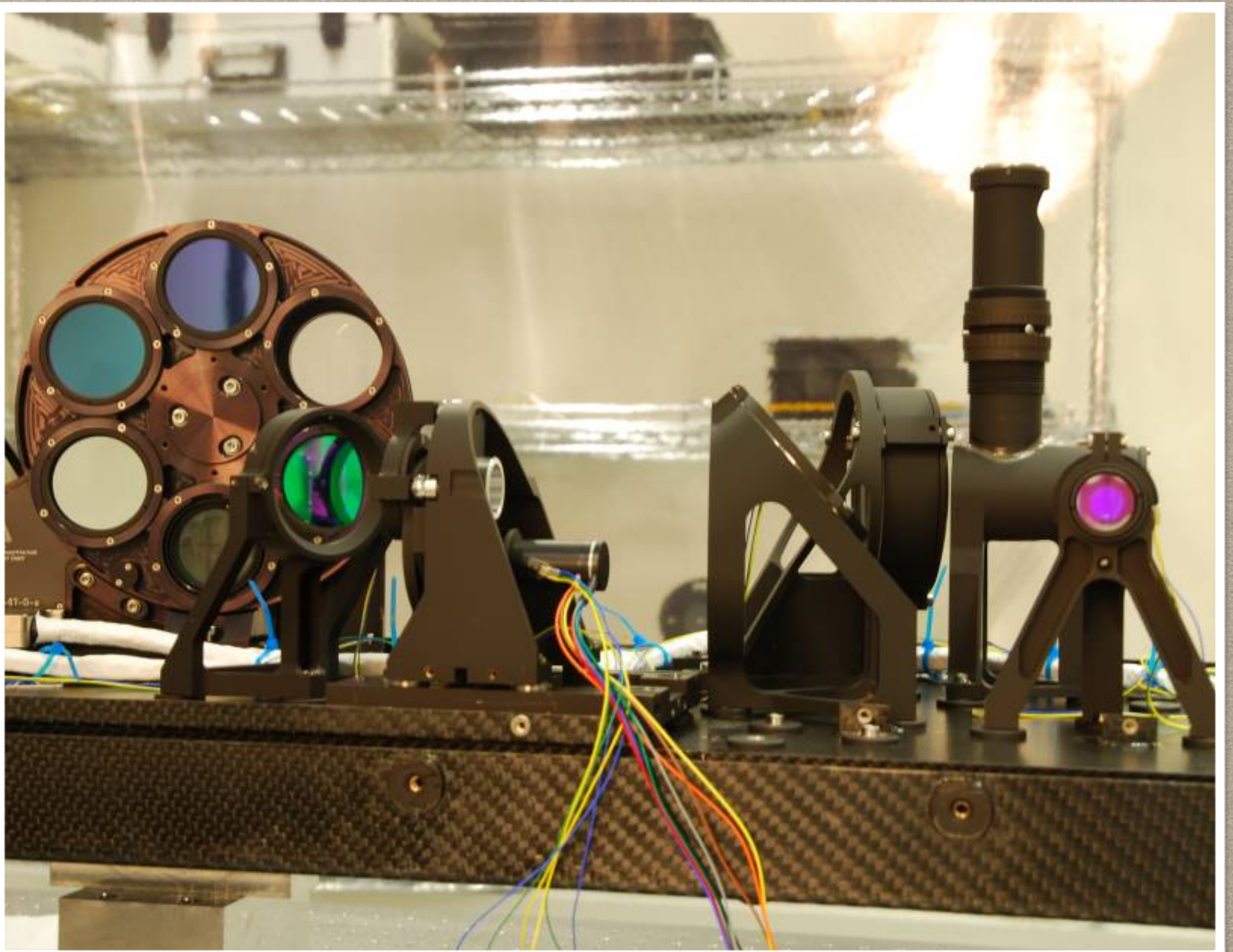
THE “OLD” SUNRISE CONFIGURATION IN 2009 & 2013

- Gondola (HAO)
 - Sun acquisition and tracking (with few tens of arcsec accuracy)
 - Power supply with solar panels and batteries
 - Carries instrument electronics, telemetry antennas and CSBF electronics
- Telescope (MPS):
 - 1 m aperture, 25 m focal length
 - Gregory configuration
 - In-flight alignment of secondary mirror for focus and coma correction



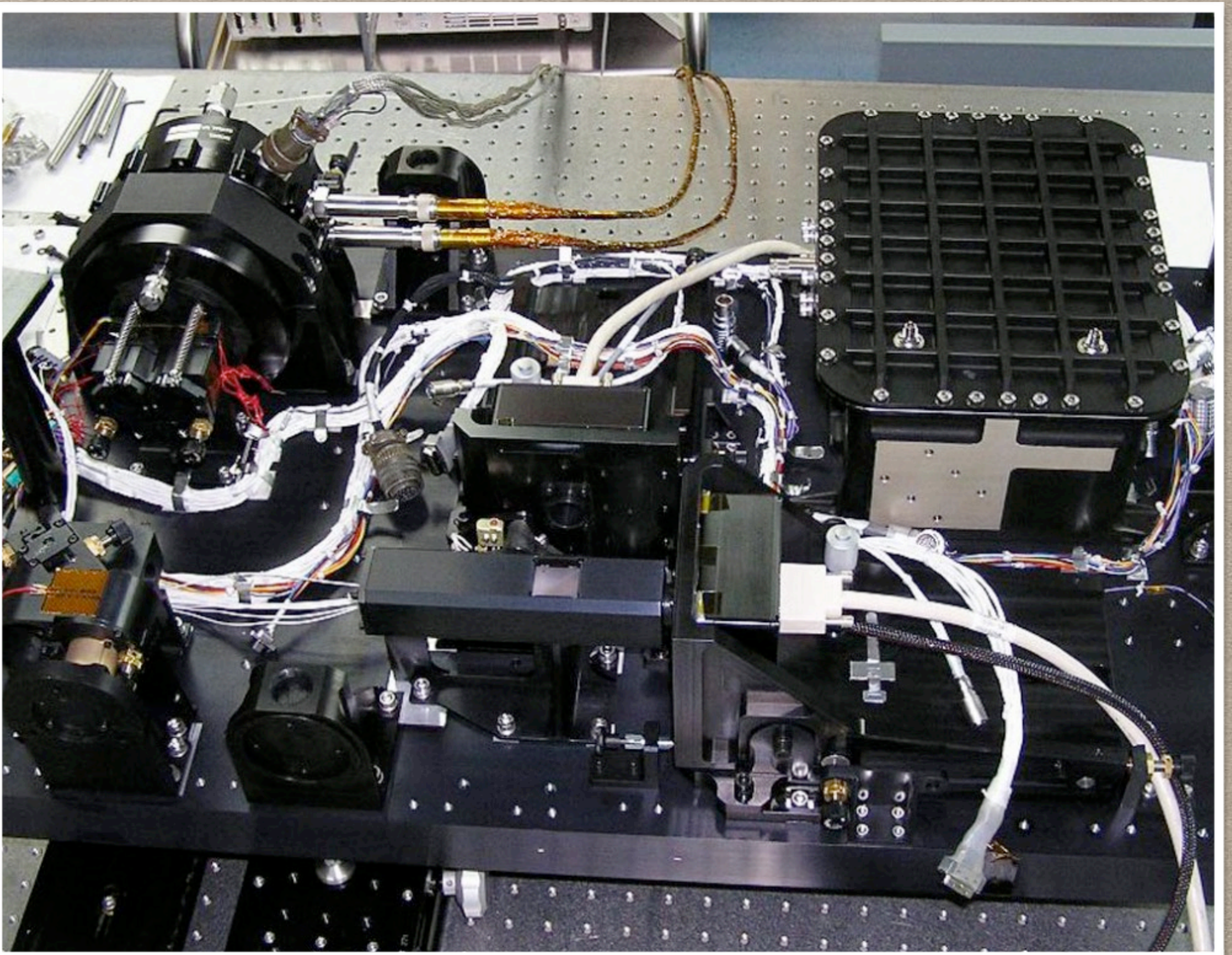
SUNRISE I+II INSTRUMENTS: SuFI

- Medium band imager with 5 λ bands
- New filter set 2013:
 - 396,84 nm (Ca II H λ , 1 λ wide)
 - 396,80 nm (Ca II d λ , 1,8 Å wide)
 - 303 nm (pseudo continuum, 4,4 nm wide)
 - 279,62 nm (Mg II b λ , 4,8 Å wide),
 - 214 nm (pseudo continuum, 22 nm wide)
- FoV: 40" x 15" with 2048 x 2048 CCD
- Phase diversity for image reconstruction
- ~ 125 m effective focal length
- 1s cadence at fixed λ , 2s for different λ

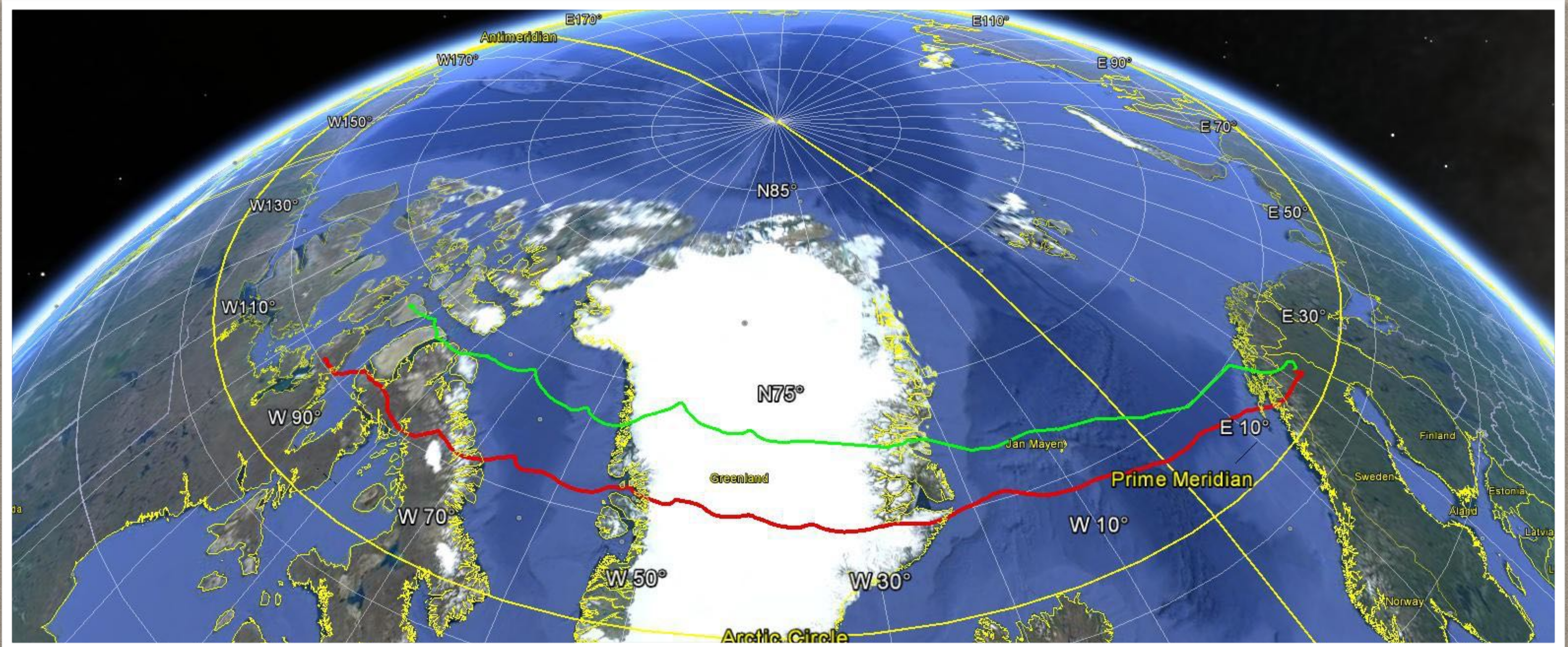


SUNRISE I+II INSTRUMENTS: IMAX

- 2D maps of magnetic vector and line-of-sight velocity
- 525.02 nm, Fe I, g=3, resolution: 85 mÅ
- Fabry-Pérot etalons, liquid crystal modulators
- FoV: 50" x 50"
- 2 CCDs 1k x 1k for phase diversity & improved polarimetry
- Full Stokes vector images every 30s
- (I,V) every 5s



SUNRISE I+II FLIGHT



No atmospheric seeing, UV spectral range accessible, continuous 24/7 observation of the Sun

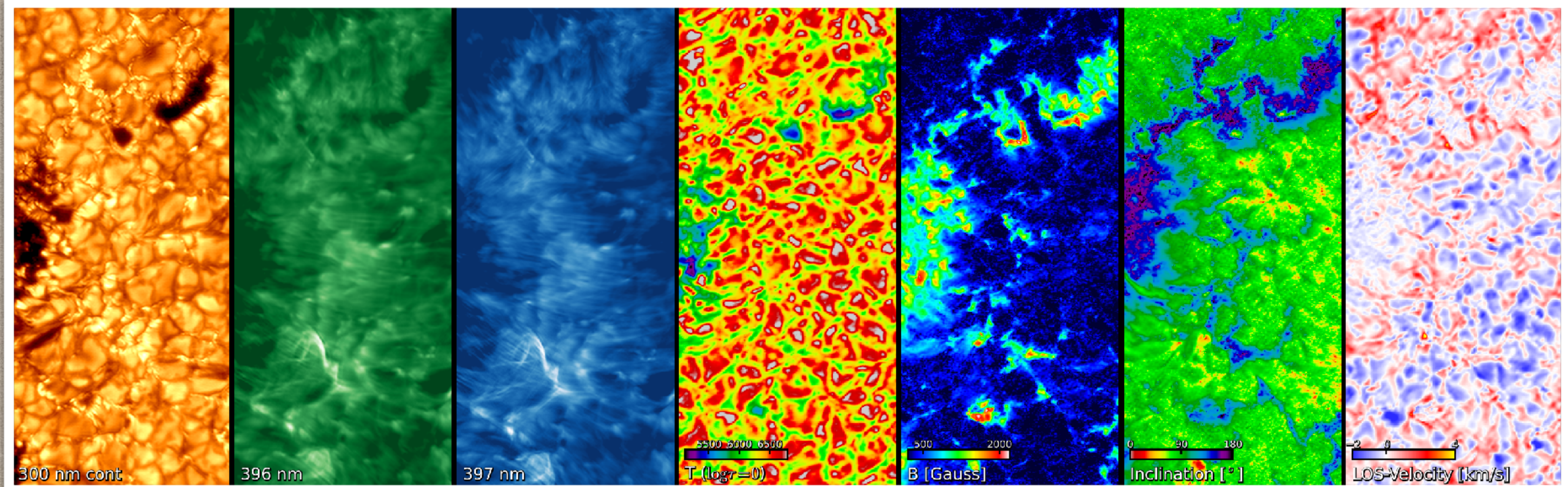
Flight termination and instrument recovery in Canada, no overflight permission over Russia for U.S. balloon



SCIENTIFIC HIGHLIGHTS

SUNRISE I+II, 2009 & 2013

SO FAR 88 REFEREED PUBLICATIONS (NOV 2017)



- First ever spatially resolved images of intense magnetic flux on the Sun show that semi-annual oscillations provide a reasonable model (Lagg et al. 2010).
- First ever brightness concentrations in the UV (171 nm) reveal very high values up to 5 above the mean quiet Sun (Riethmüller et al. 2010).
- First ever measurements of the contrast of granulation in the UV up to 30%, consistent with theory. These values provide the efficiency of convective energy transportation (Hirzberger et al. 2010).
- First determination of elements directionality from sampling different parts of the magnetic field contrast to investigate whether they were close to horizontal or strongly affected by the solar rotation.
- Ubiquitous small-scale whirl flows are found which drag small-scale magnetic field structures into their centres (Bonet et al. 2010).
- Magnetic field extrapolations from SUNRISE/IMaX data indicate that most magnetic loops in the quiet Sun remain within the photosphere. Only a small fraction reaches the chromosphere. The loops are strongest in mesogranular lanes, although there is no particular mesogranular scale (Yelles Chaouche et al. 2011).
- Discovery that 85 % of the internetwork magnetic fields stronger than 100 G are concentrated in mesogranular lanes, although there is no particular mesogranular scale (Yelles Chaouche et al. 2011).

GONZALEZ et al. 2011, REQUERIO et al. 2011.

SUNRISE II SCIENCE HIGHLIGHTS (SOLANKI ET AL., 2017)

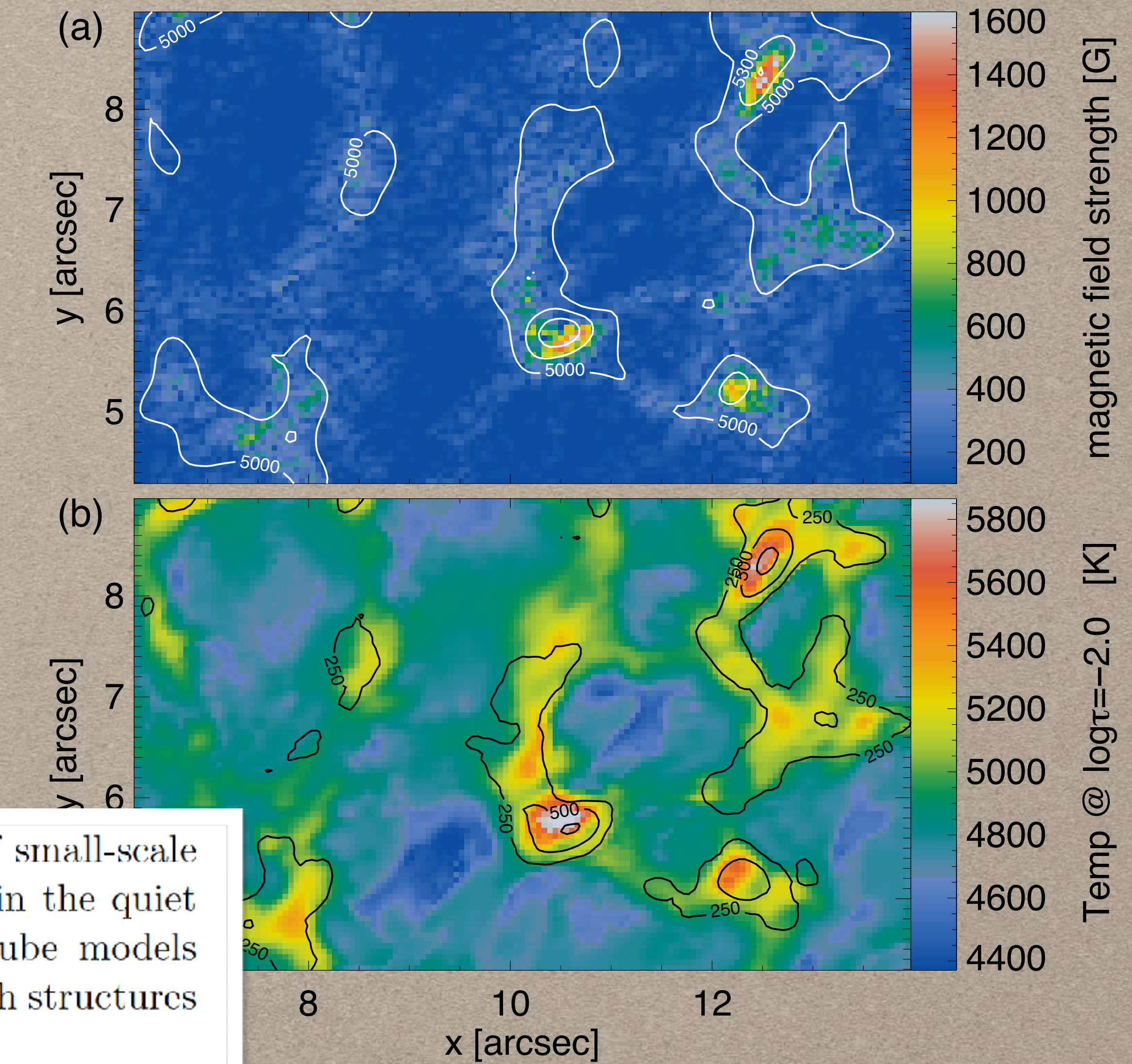
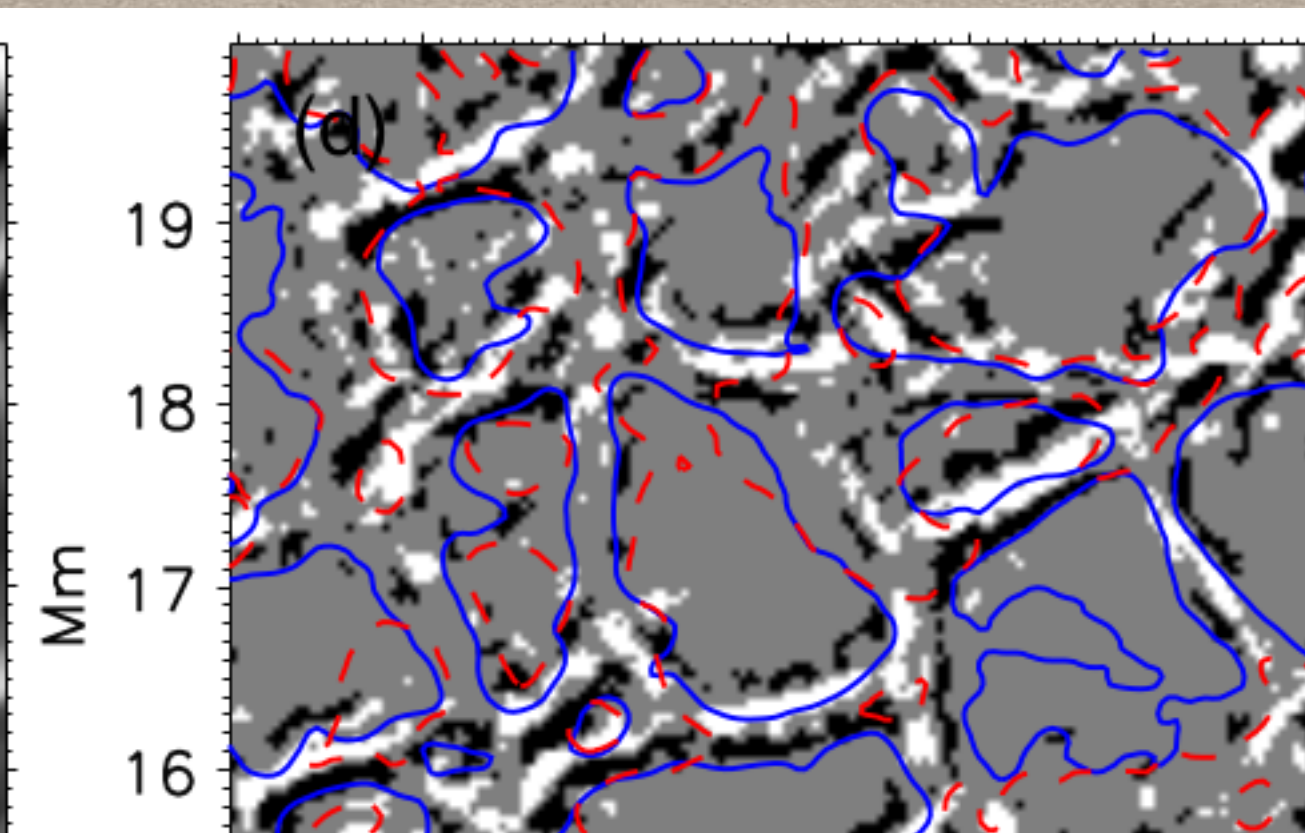
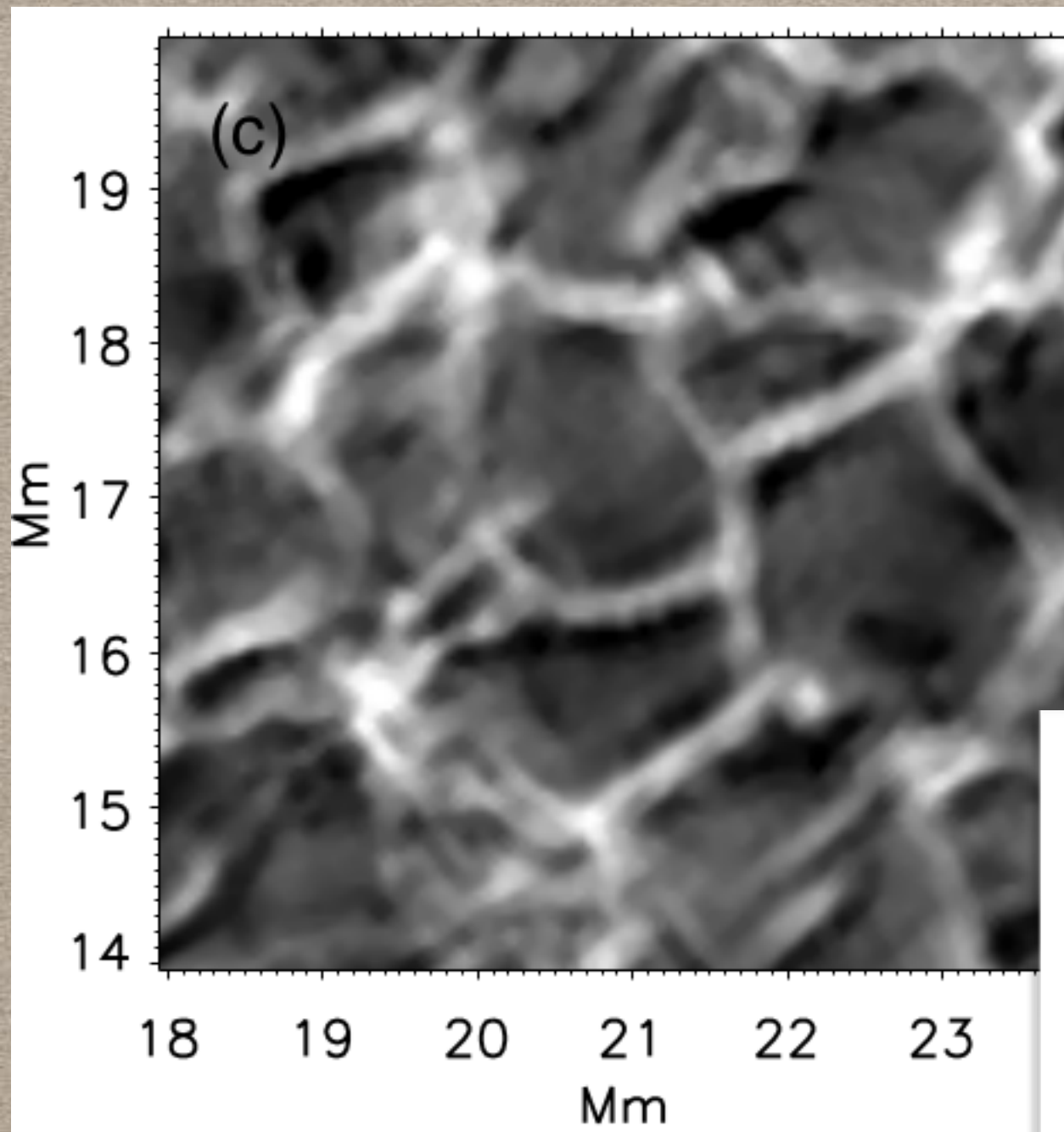
1. [Centeno et al. \(2017\)](#) analyzed emerging the interrelated dynamics of the gas and reports on two emerging flux events, do possible the interrelated dynamics of the occurrence of magnetic reconnection due to the interaction of the magnetic field with the solar plasma.
2. The properties of a likely siphon flow connecting magnetic elements with a polarity inversion line are determined from the 3D structure of the magnetic field.
3. The problem of the low contrast of the large-scale magnetic fields is addressed by contrasting the observations with numerical simulations.
4. The problem of the origin and of the physical difference between superdiagonal and extreme superdiagonal magnetic fields is addressed by comparing the observations with numerical simulations.
5. The discovery of ubiquitous transverse waves travelling along these fibrils and carrying copious amounts of energy is reported by [Jafarzadeh et al. \(2017\)](#), while [Gafeira et al. \(2017a\)](#) present the discovery of compressible waves travelling along the fibrils, which they interpret as a canopy of magnetic field lines.
6. [Jafarzadeh et al. \(2017\)](#) compare the observations with numerical simulations of the magnetic field and gas using the SUNRISE II/IMaX observations as a boundary condition. In this way they obtain the magnetic field structure in the upper atmosphere without having to assume the validity of the force-free assumption in the solar photosphere. They computed linear magneto-static equilibria for all the IMaX frames of the active region, without the problems faced when modeling the magnetic field in different atmospheric layers of the quiet Sun.
7. [Wiegmann et al. \(2017\)](#) have computed general linear magneto-static equilibria of the magnetic field and gas using the SUNRISE II/IMaX observations as a boundary condition. In this way they obtain the magnetic field structure in the upper atmosphere without having to assume the validity of the force-free assumption in the solar photosphere. They computed linear magneto-static equilibria for all the IMaX frames of the active region, without the problems faced when modeling the magnetic field in different atmospheric layers of the quiet Sun.
8. [Chitta et al. \(2017\)](#) observed that coronal loops are rooted in opposite polarity fields. They provide evidence for flux cancellation at Y-shaped jets (signatures of magnetic reconnection) at the footpoints that might supply (hot) plasma to the overlying coronal loops. This challenges the traditional picture in which each loop footpoint is located in a unipolar region on the solar surface.
9. [Kahil et al. \(2017\)](#) probe the relationship between brightness contrast at UV and visible wavelengths and the magnetic flux in the quiet Sun, finding that the contrast keeps increasing with magnetic flux, unlike most earlier observational results, but in qualitative agreement with MHD simulations.
10. [Danilovic et al. \(2017\)](#) compare an Ellerman bomb observation with a similar, simulated event in which magnetic reconnection is triggered by the emergence of emerging flux. The 3D radiation-MHD simulation reproduces the underlying physical process and the limitations of the observations. The SUNRISE/IMaX data cannot determine the height at which the reconnection takes place. The authors also show, however, that the velocity vectors measured at the high resolution of SUNRISE/IMaX reveal that the MHD simulations can be overcome.
11. [Jafarzadeh et al. \(2017\)](#) characterize the wave modes observed at two heights in magnetic bright points, including both compressible waves seen in brightness fluctuations and transverse waves obtained from proper motions.
12. The short travel times suggest large wave speeds. A new estimate of the flux emergence rate in the quiet Sun is obtained by [Smitha et al. \(2017\)](#). Compared with the emergence rate deduced from Hinode/SOT data using the same technique, the emergence rate obtained from SUNRISE I data is around an order of magnitude larger.

SUNRISE I: RESOLVING SMALL-SCALE STRUCTURES



Lagg et al., 2010; Martínez González et al 2012, Requerey et al. 2015

Granular flows Khomenko et al. 2010

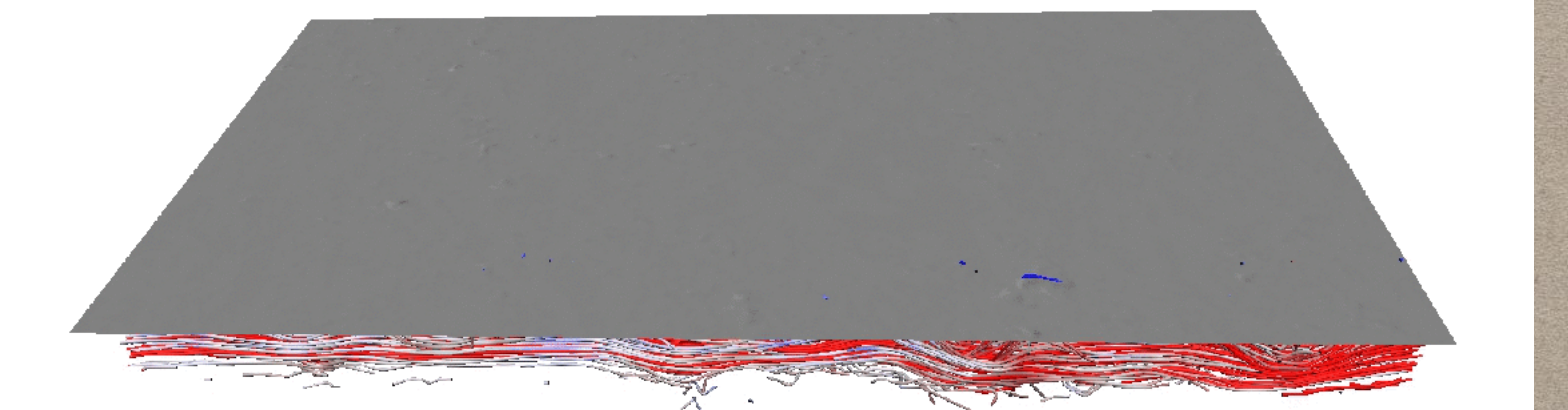
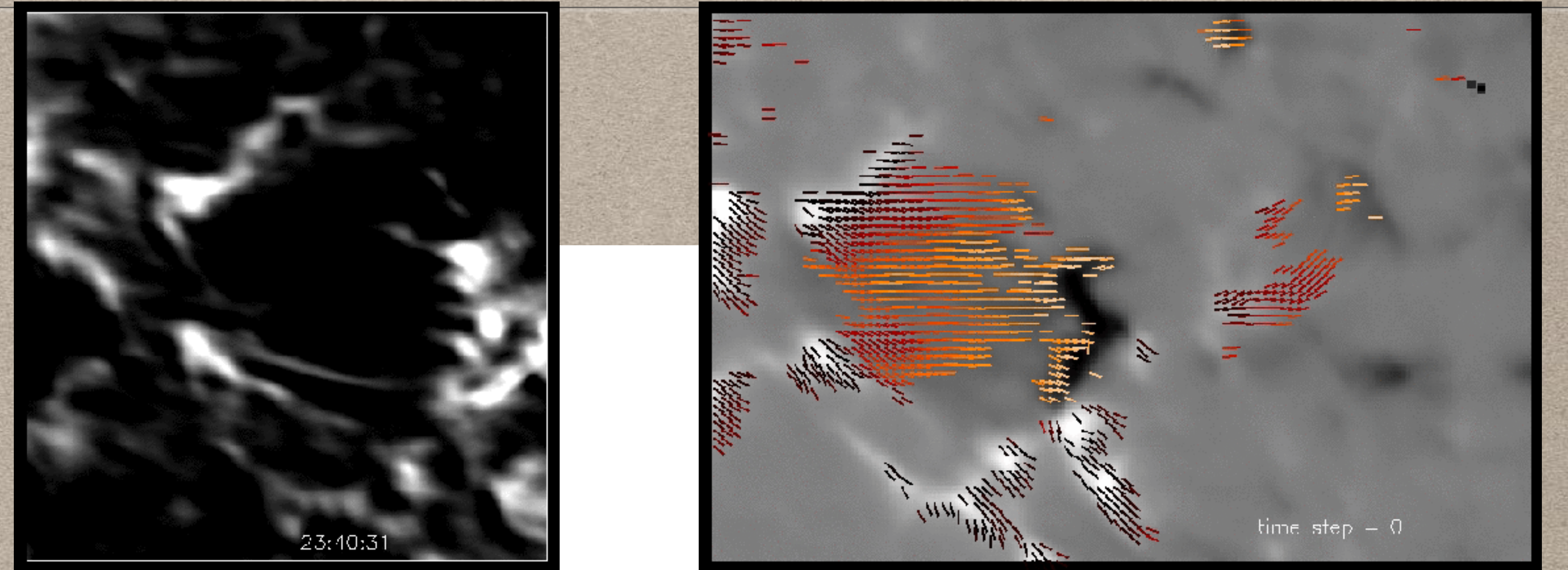


- First ever spatially resolved images of small-scale intense magnetic flux concentrations in the quiet Sun show that semi-empirical flux tube models provide a reasonable description of such structures (Lagg et al. 2010).

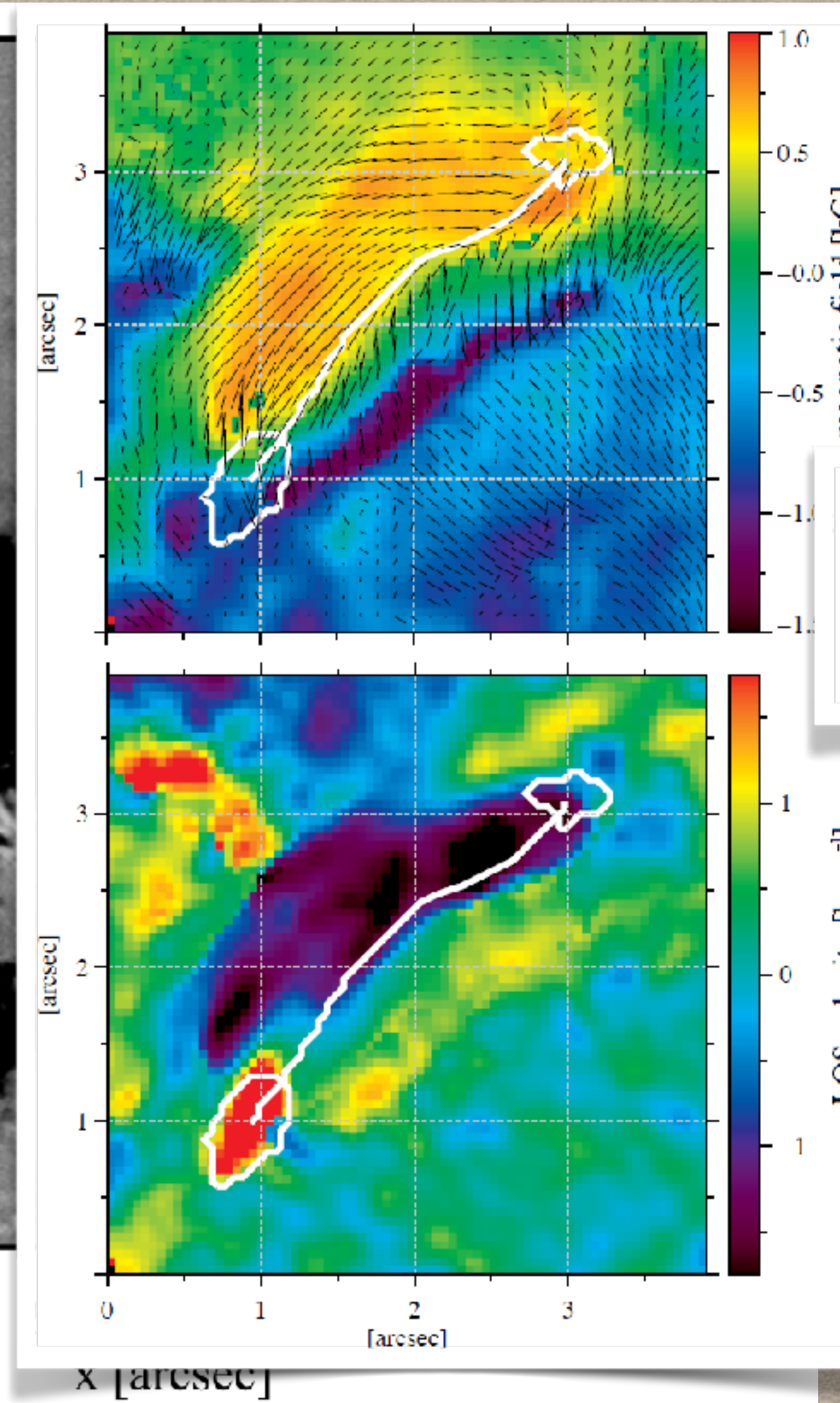
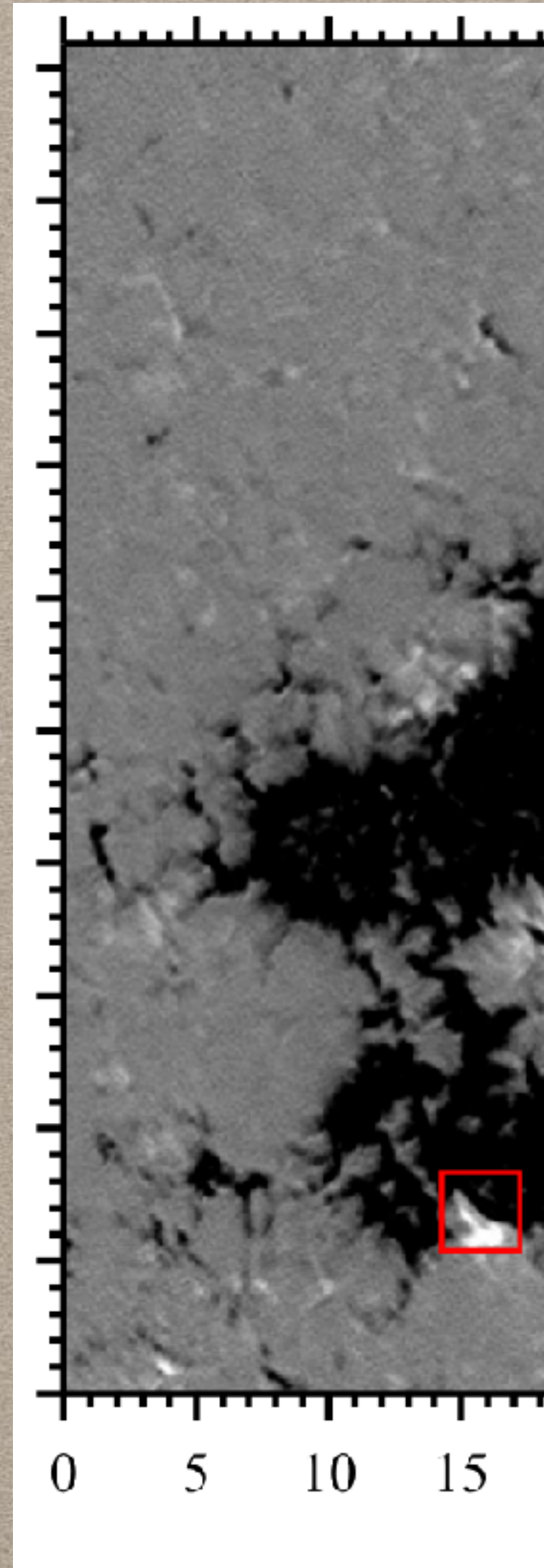
AN ACTIVE REGION CLOSE-UP



Centeno et al. 2017;
Requerey et al. 2017;
Danilovic et al. 2017:
IMaX uncovers the
dynamics and
topology of
emerging flux
regions. The vector
magnetic field is used
to trace magnetic
field lines

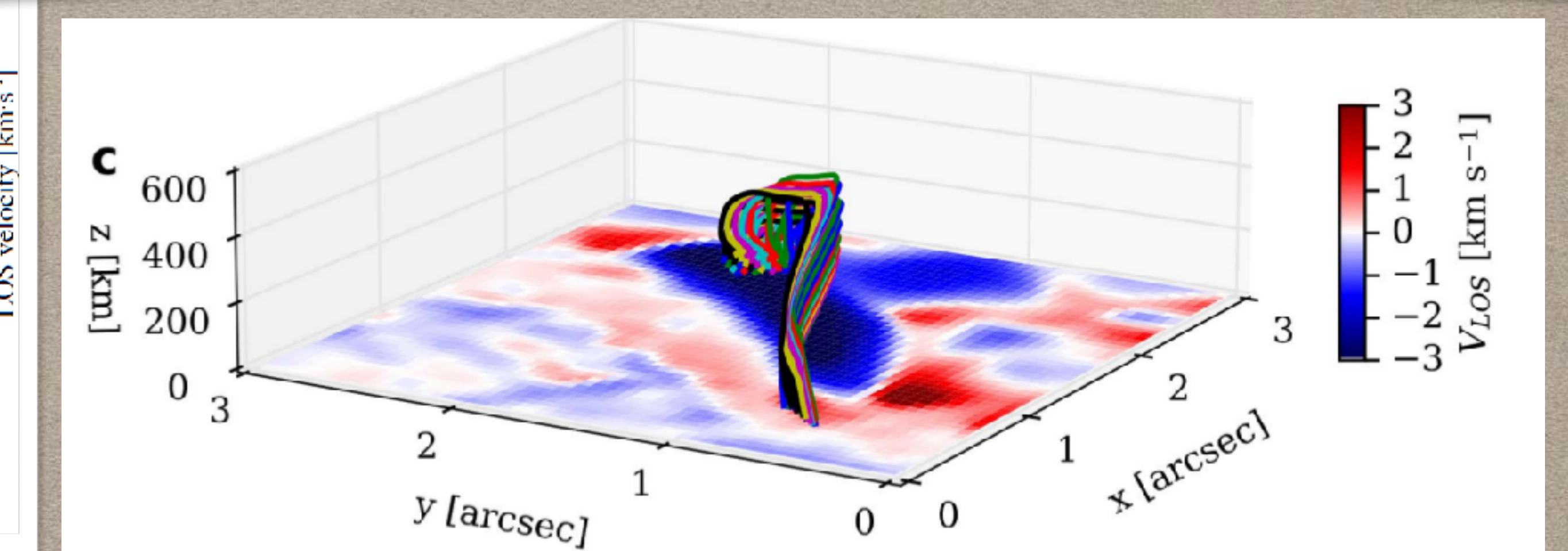


1. [Centeno et al. \(2017\)](#) analyzed emerging flux regions with a detailed description of the interrelated dynamics of the gas and the field, including the reports on two emerging flux events, describing in greater detail than previously possible the interrelated dynamics of the gas and the field, as well as the likely occurrence of magnetic reconnection during the emergence.



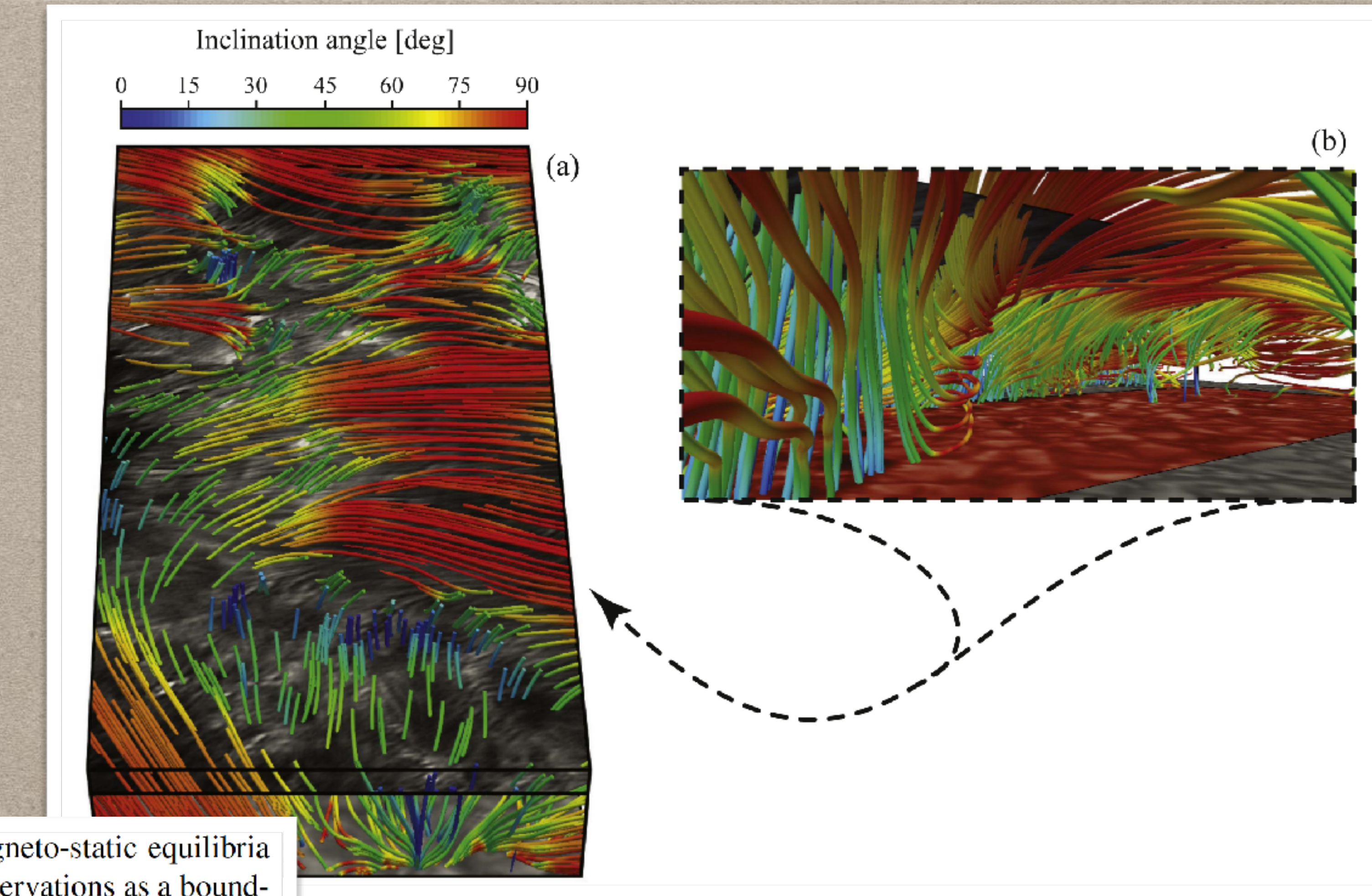
Requerey et al. 2017:
 A magnetic flux concentration with a weak field of positive polarity and displaying an upflow is connected by a set of arch-shaped magnetic field lines with a strong field patch of negative polarity showing a downflow

2. The properties of a likely siphon flow and of the small, initially low-lying loop connecting magnetic elements with a pore are deduced by Requerey et al. (2017a) and the 3D structure of the magnetic field lines and hence of the flow vector are determined.



MAGNETIC FIELD LINES & FIBRILS

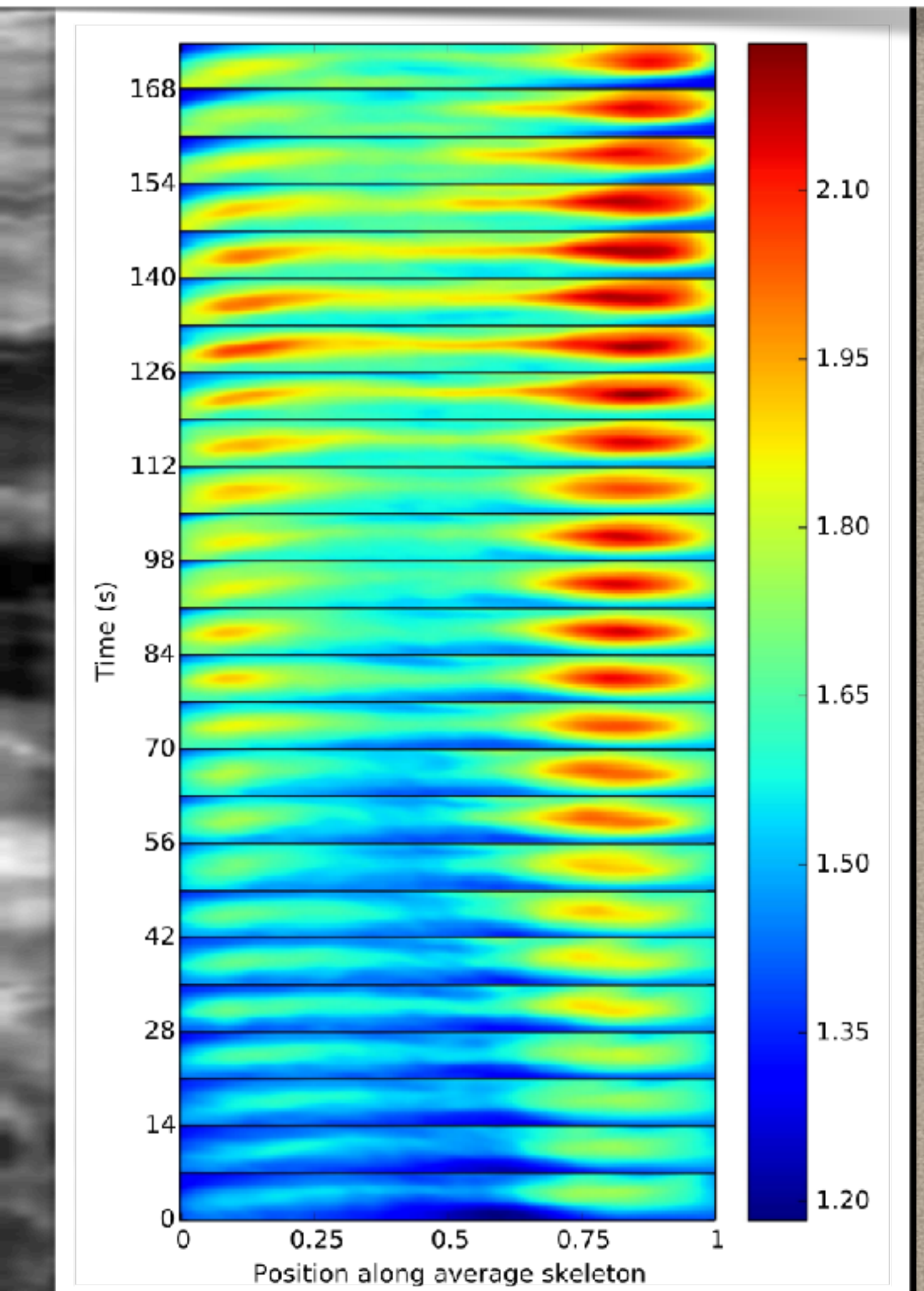
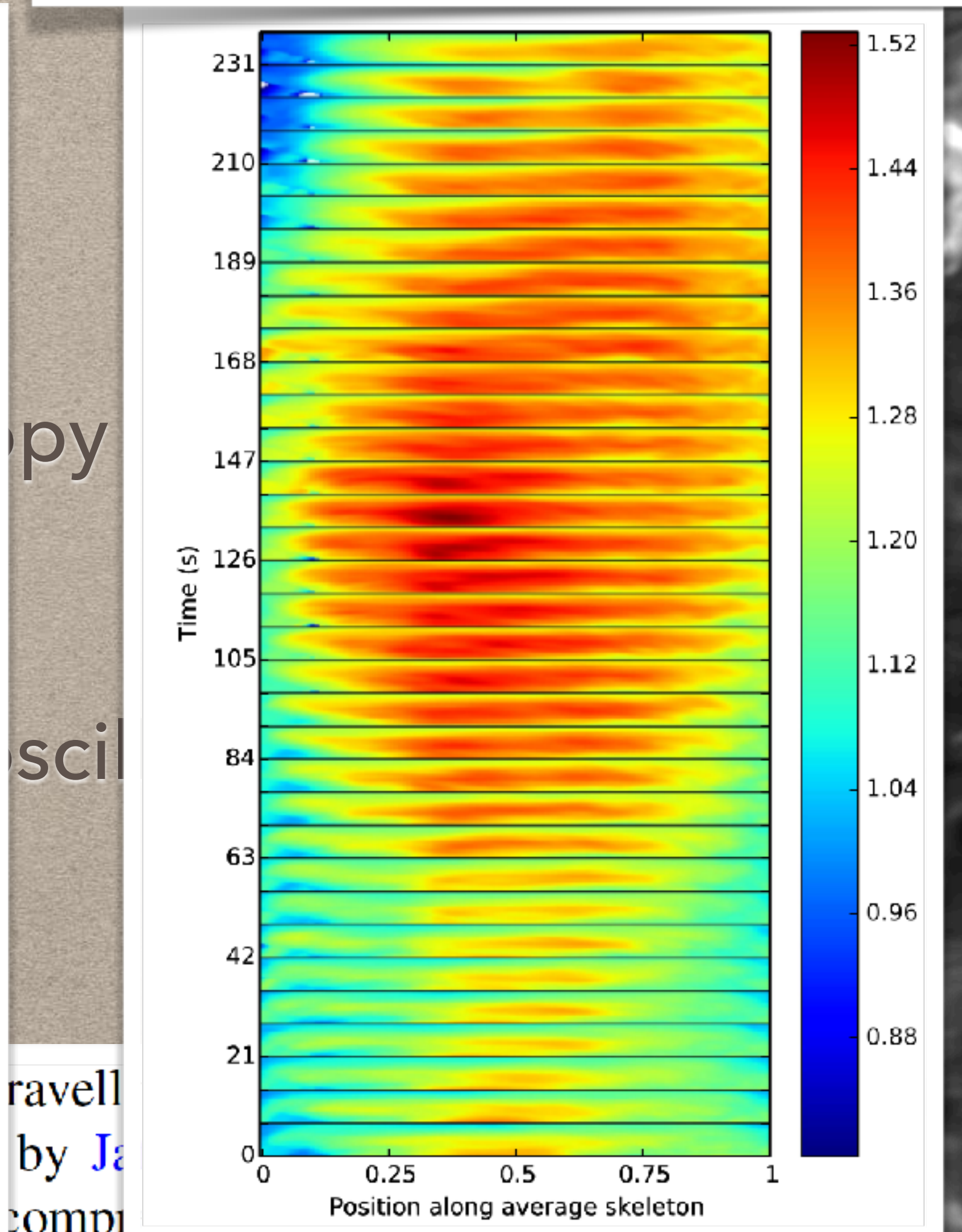
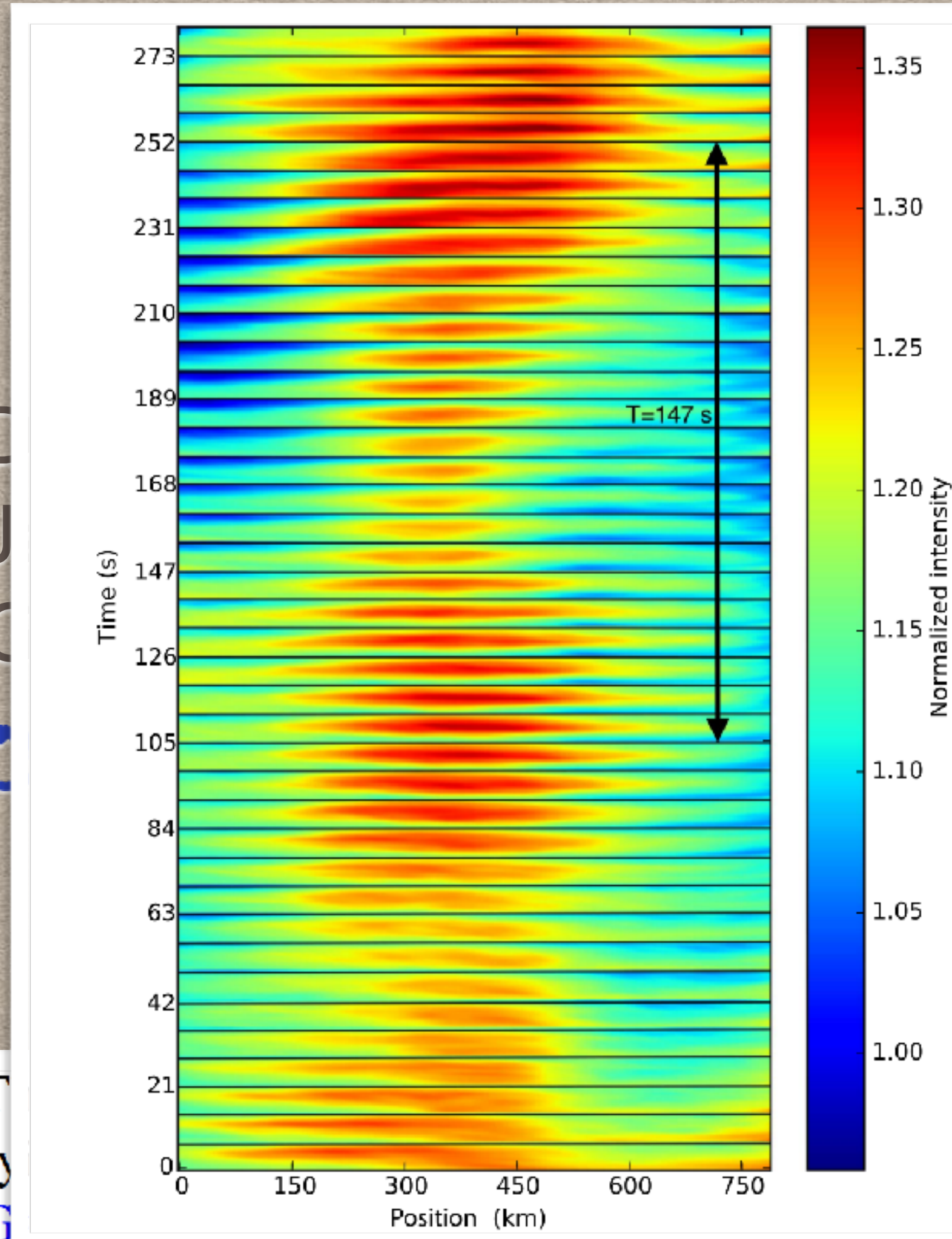
- Wiegelmann et al. 2017:
Compute magnetostatic equilibrium from Spinor inversions of IMaX data.
More reliable in lower atmosphere than force free fields



11. [Wiegelmann et al. \(2017\)](#) have computed general linear magneto-static equilibria of the magnetic field and gas using the SUNRISE II/IMaX observations as a boundary condition. In this way they obtain the magnetic field structure in the upper atmosphere without having to assume the validity of the force-free assumption in the solar photosphere. They computed linear magneto-static equilibria for all the IMaX frames of the active region, without the problems faced when modeling the magnetic field in different atmospheric layers of the quiet Sun.

SLENDER CA FIBRILS

6. The properties of the slender fibrils dominating the SuFI Ca II H images are determined by Gafeira et al. (2017b), who show that the fibrils live much longer than a simple analysis would suggest, if one takes into account that they often fade away and reappear after some time.



the fibrils, which they identify as sausage waves.

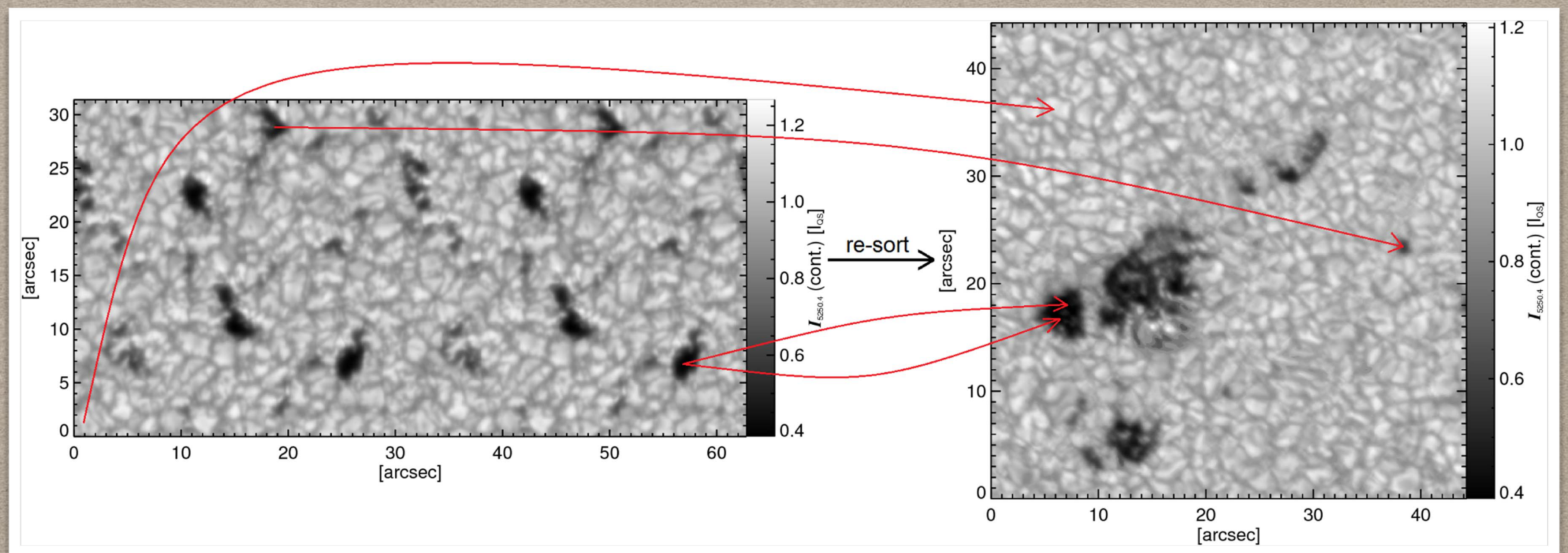
(1) MHD cube with QS, plage, pores: compute Stokes vector

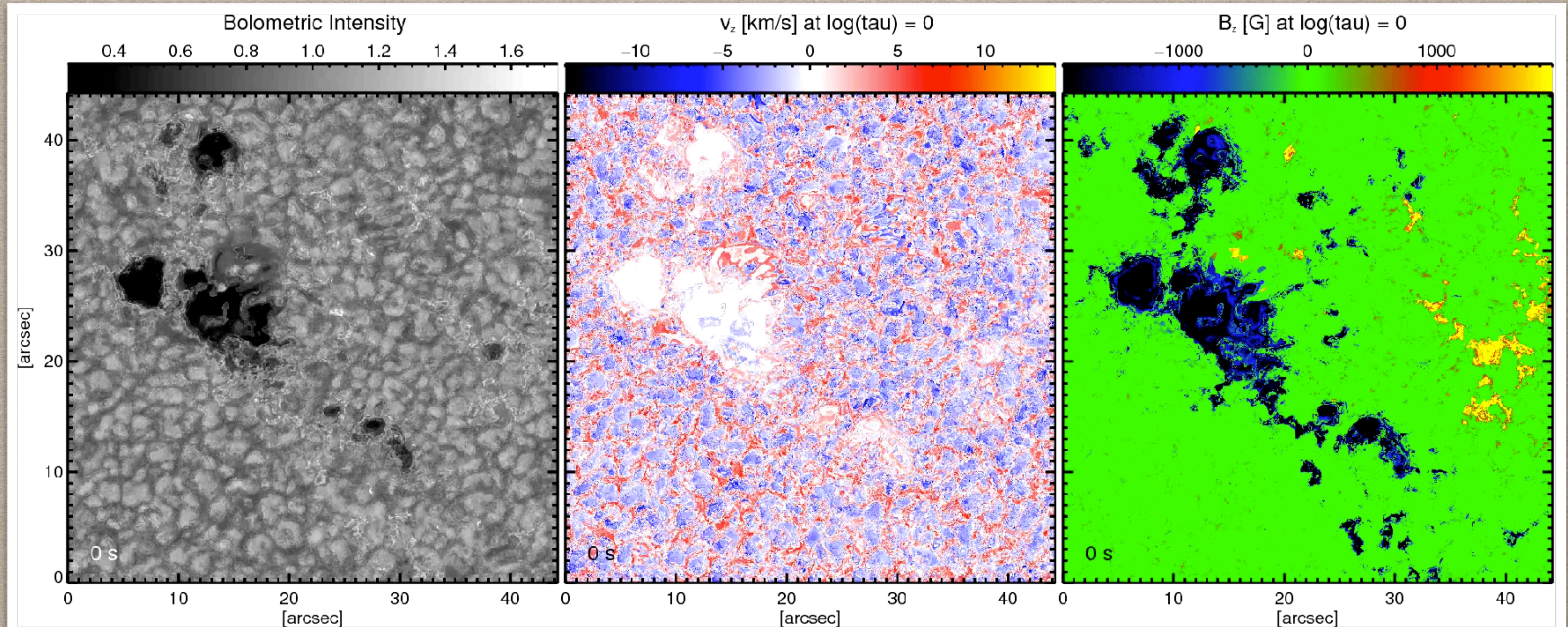
(2) degrade (spatial & spectral) according to instrument

(3) in every pixel: assume the atmosphere corresponds to the MHD atmosphere of the best matching Stokes profile

(4) use this (inconsistent) MHD cube as initial condition for an MHD run

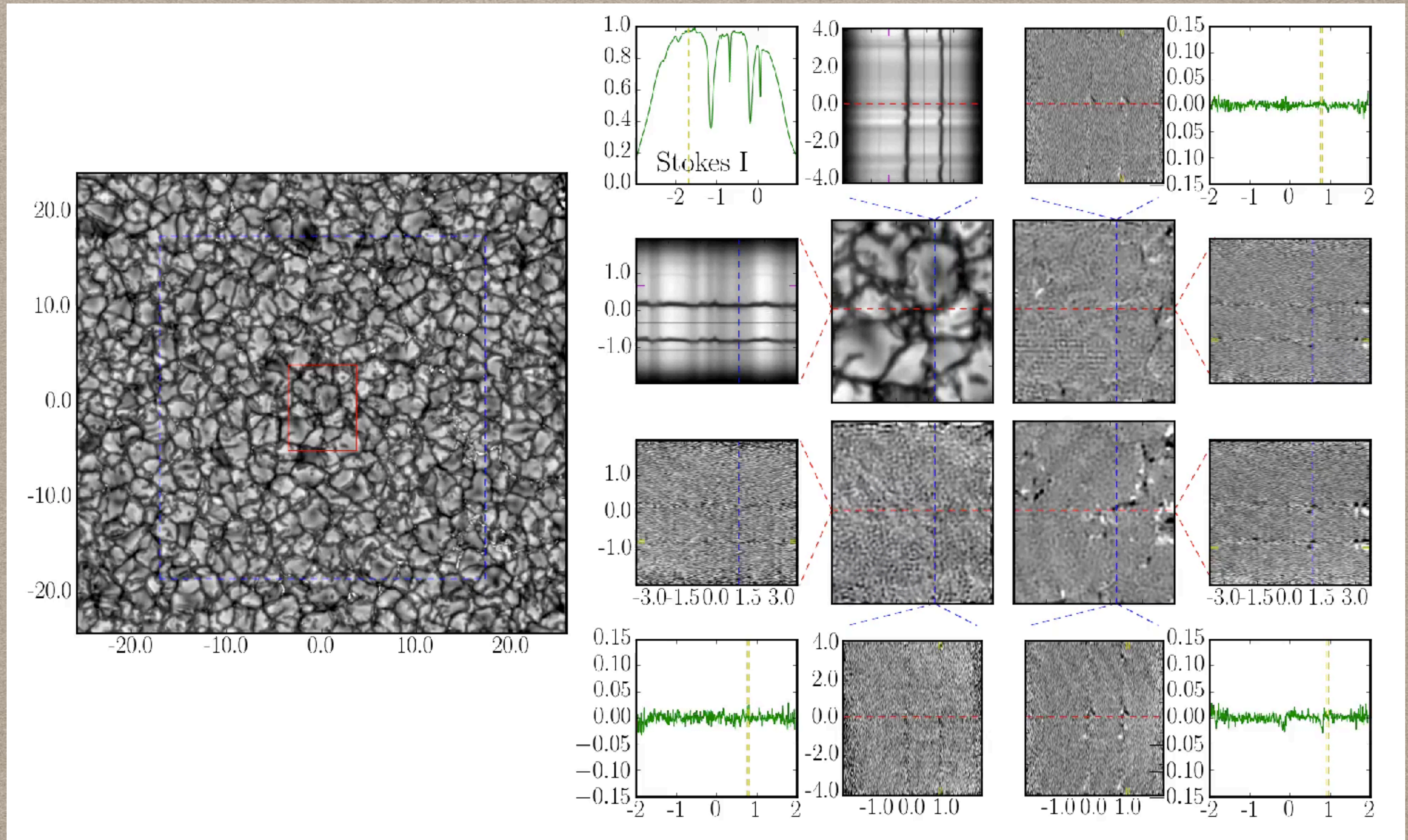
(5) repeat (3)-(4) until MHD relaxes



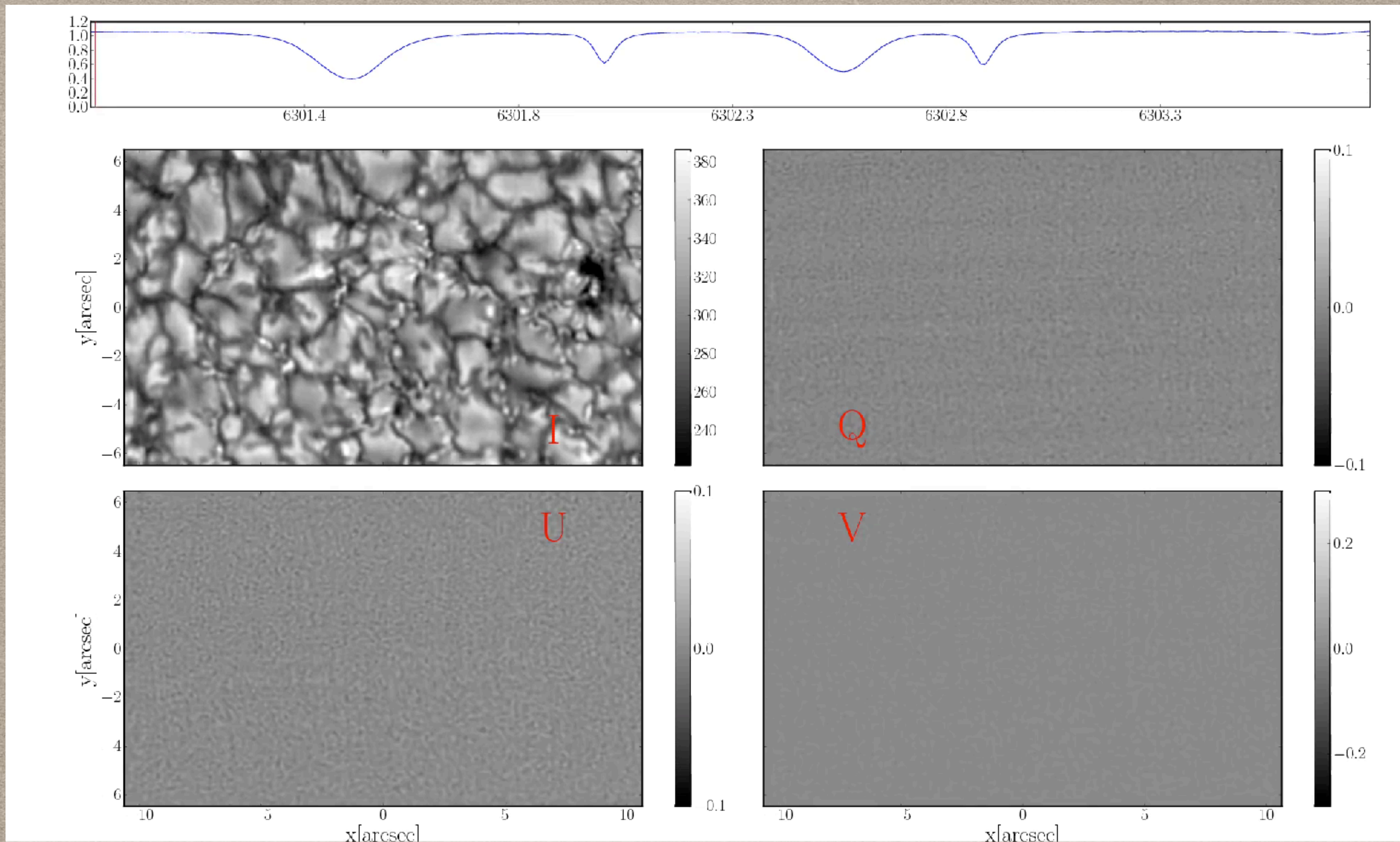


5. Riethmüller et al. (2017) present a novel inversion technique employing magnetohydrodynamic (MHD) simulations to provide the model atmospheres needed to compute synthetic Stokes vectors that reproduce the observed Stokes parameters. They illustrate the quality of the inversions by applying the technique to the SUNRISE II polarimetric data.

EXCURSION 1: MIHI



EXCURSION 2: SPECTRAL RECONSTRUCTION

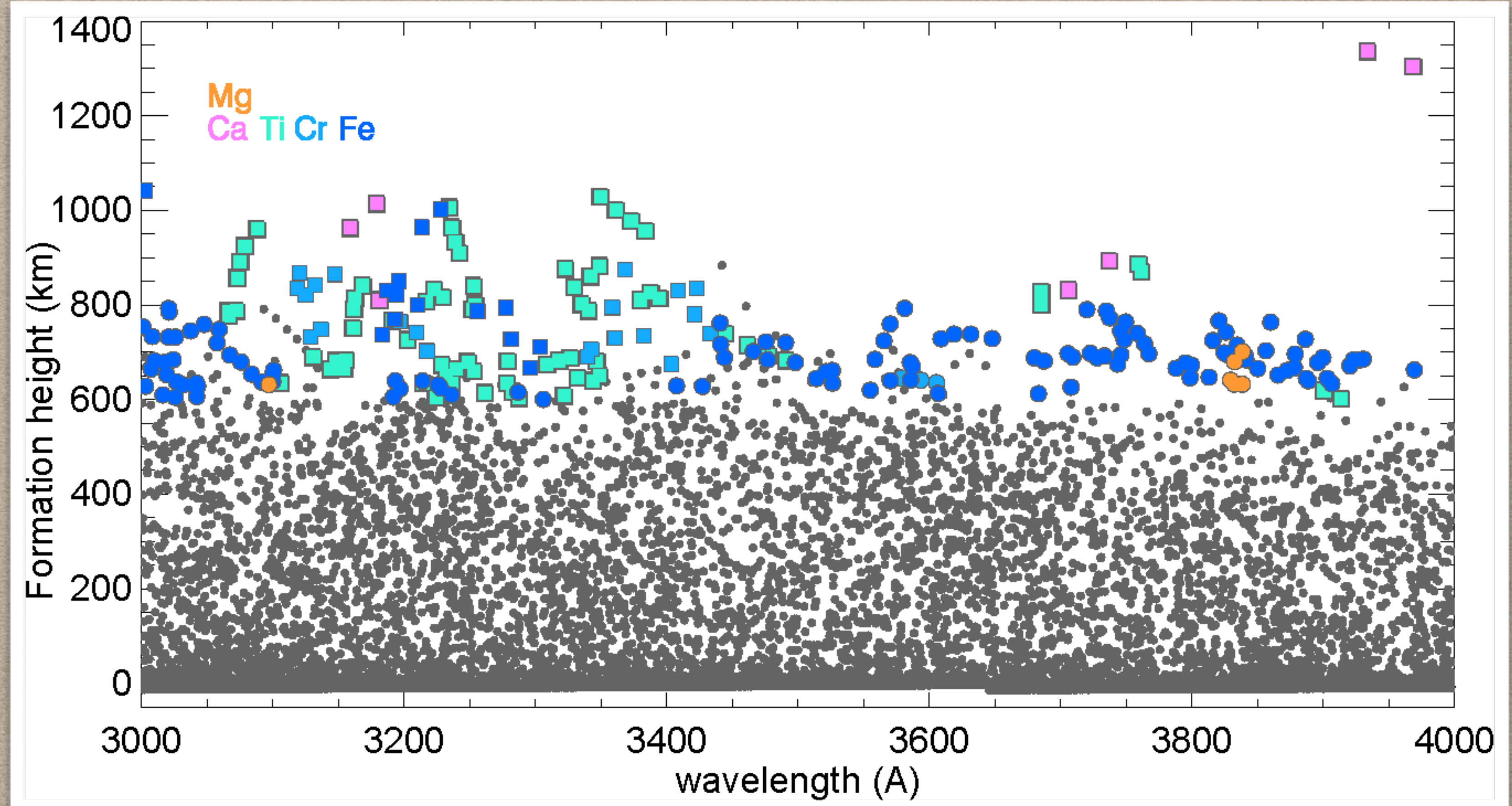


WHY SUNRISE III?

A 1-M TELESCOPE IN THE DKIST ERA?

WHERE COULD SUNRISE III DO BETTER THAN DKIST?

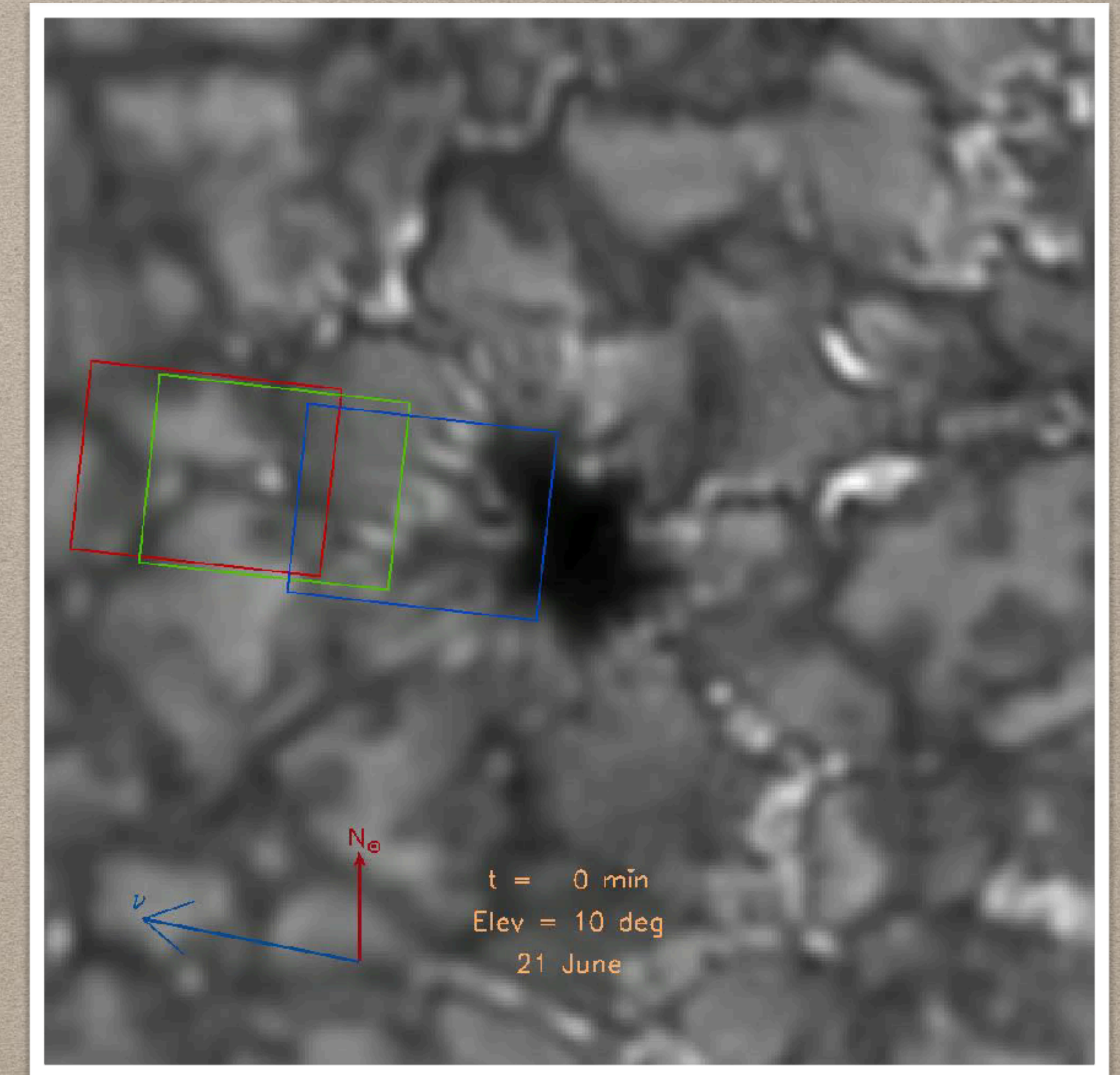
- Spectral region: UV
- Seeing-free environment
- no atmospheric refraction
- well-known PSF
- high pol. S/N ratio (no noise increase from reconstruction)
- no telluric lines
- long time series



ATMOSPHERIC DISPERSION

- DL-NIRSP high-resolution field
 $1.8'' \times 2.4''$
- channels:"
 - **8542 Å**
 - **10830 Å**
 - **15000 Å**

(K. Reardon)



THE NEW SUNRISE

EXPLOITING THE 3RD DIMENSION



SUNRISE Re-Flight 2020:
Seeing the Sun with new Eyes

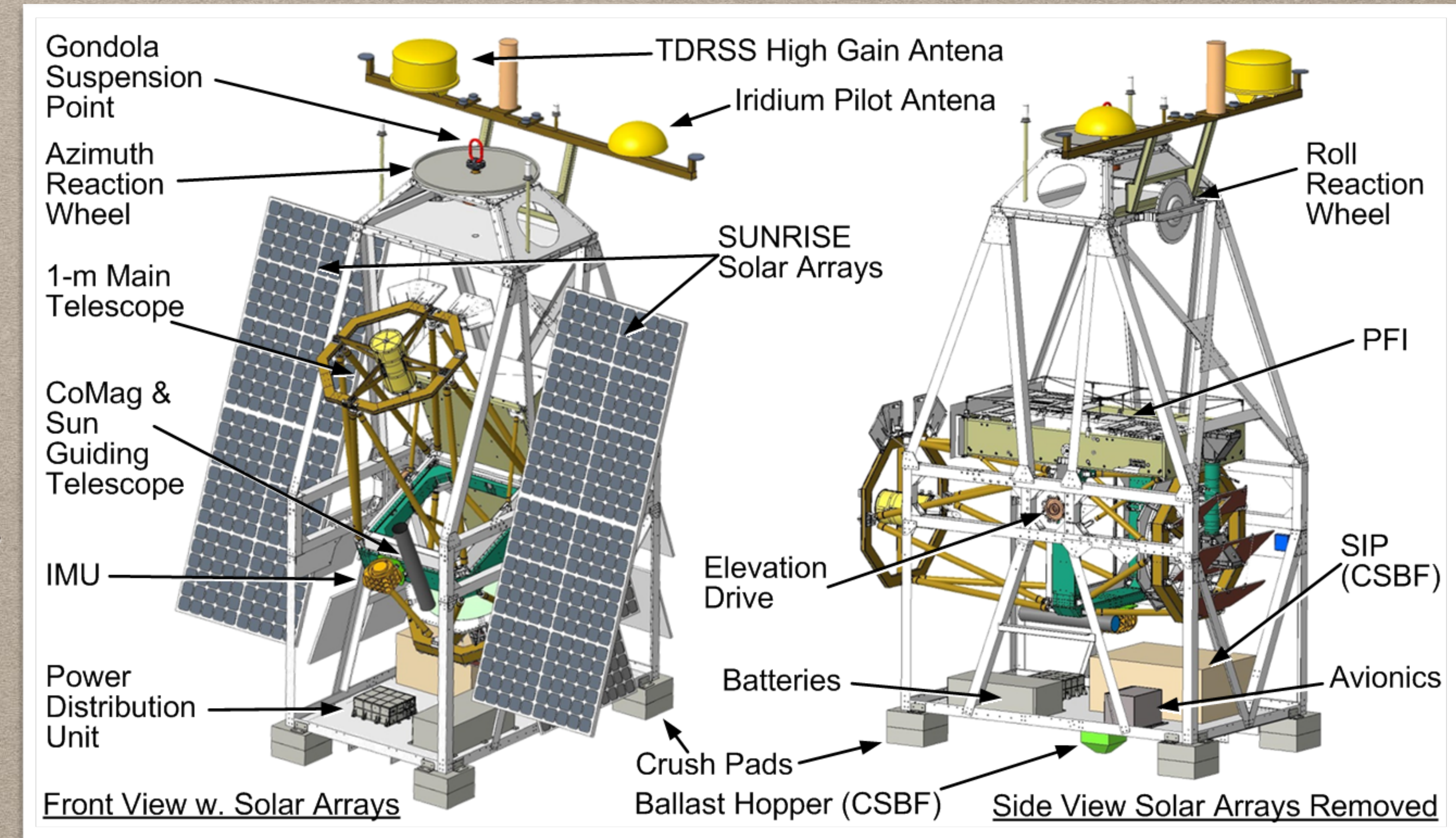


Sami K. Solanki and the SUNRISE team

Max-Planck-Institut für
Sonnenforschung
Justus-von-Liebig-Weg 3
37077 Göttingen

THE "NEW" SUNRISE

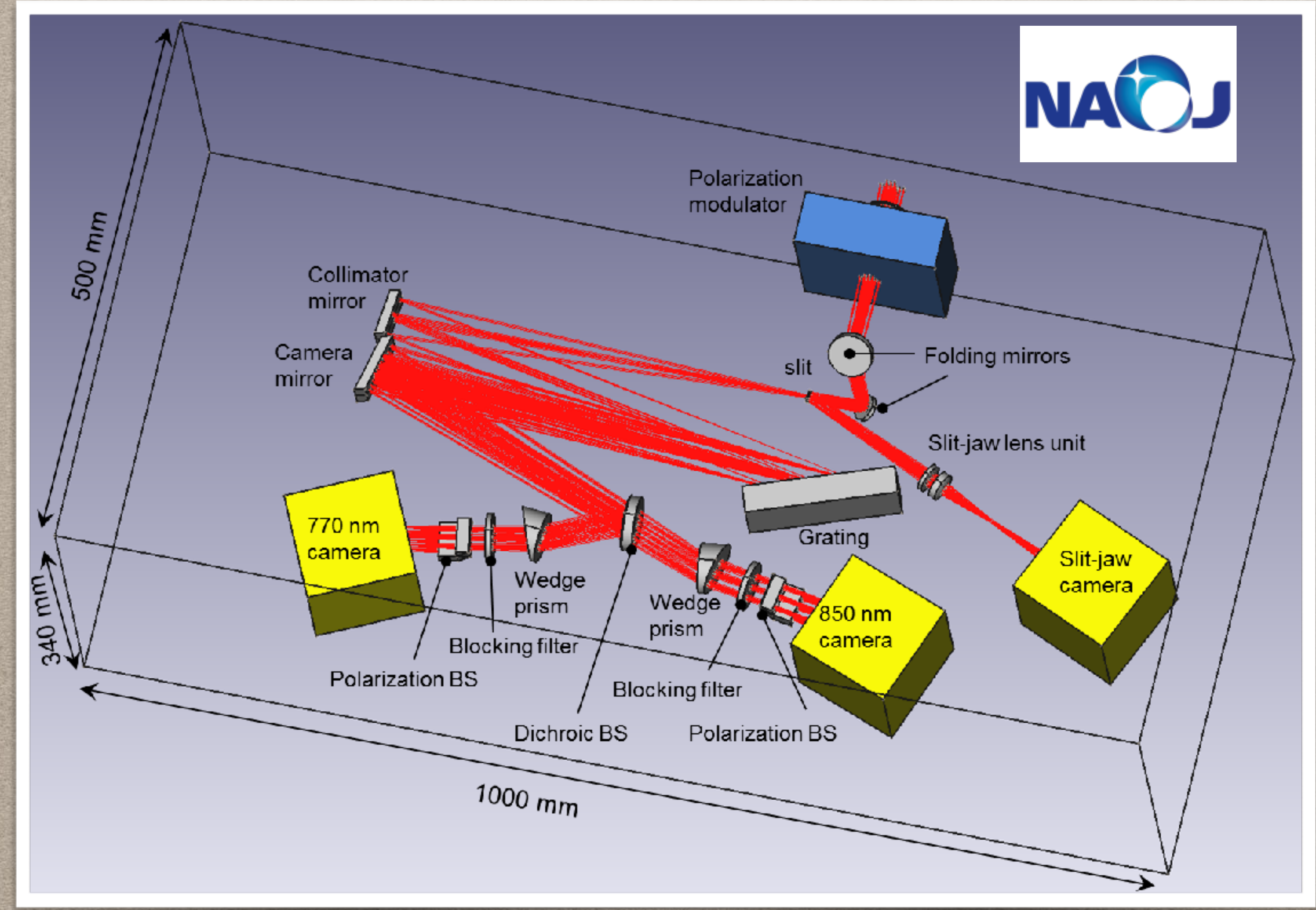
- new gondola (APL): now with roll damping
- new instruments:
 - Chromospheric Infrared Spectropol. (SCIP)
 - UV Spectropol. & Images (SUSI)
- refurbished IMaX+



SUNRISE CHROMOSPHERIC INFRARED SPECTRPOL (SCIP)



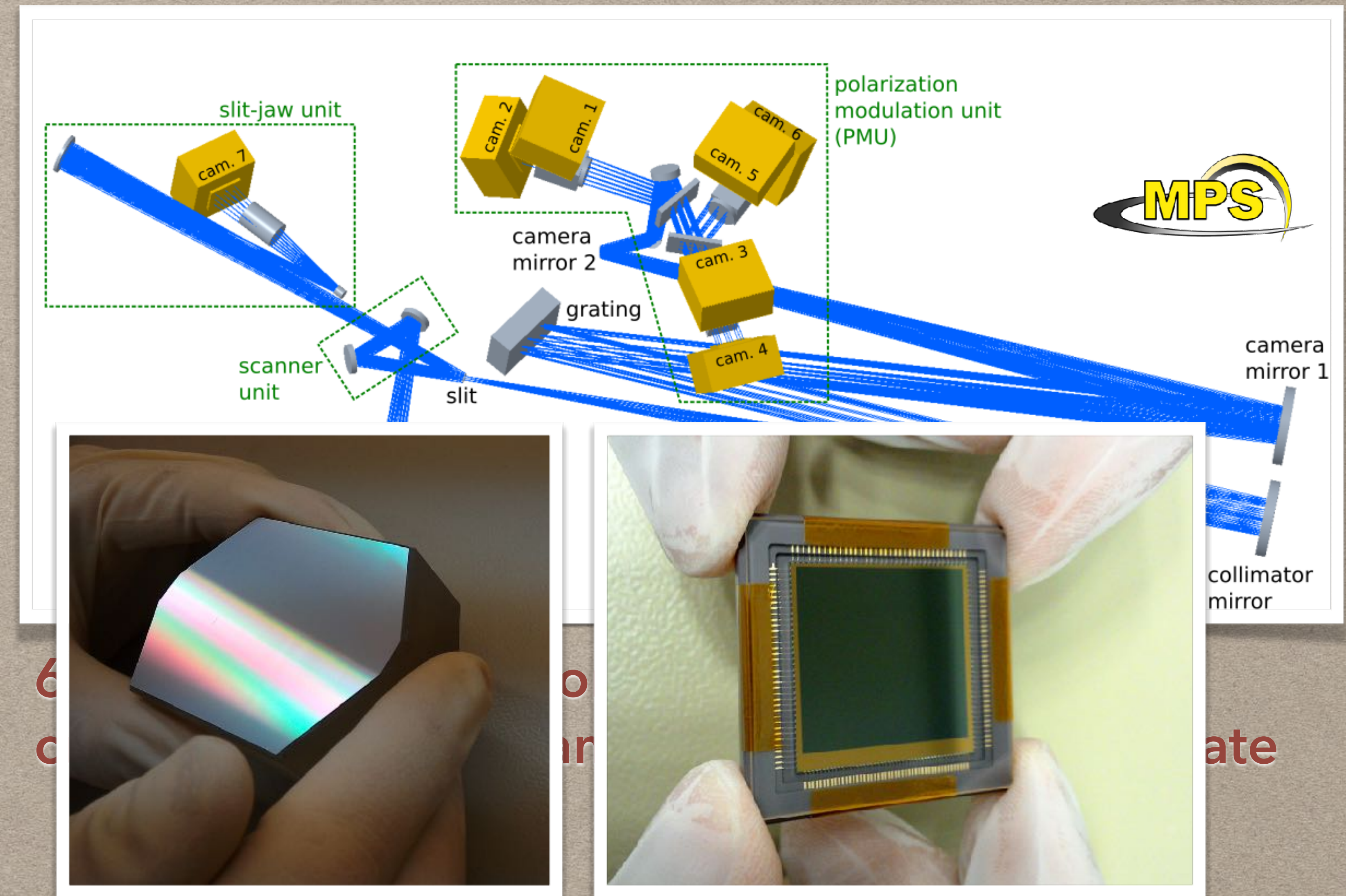
Spectral range	765 - 855 nm
Optical scheme	Littrow spectrograph with Echelle grating and off-axis aspherical mirror, slit scan unit and slit-jaw imager
Scientific target, wavelength bands	Photosphere: Fe I 846.8 nm, Fe I 851.4 nm Upper photosphere: K I 766.5 nm, K I 769.9 nm Chromosphere: Ca II 849.8 nm, Ca II 854.2 nm
FOV	58" x (61 - 83) Å
sampling	0.094" x (39 - 42) mÅ/px
Cadence	1 - 10 s
Max. pol. accuracy	3×10^{-4}



NAOJ

SUNRISE UV SPECTROPOL. AND IMAGER (SUSI, MPS)

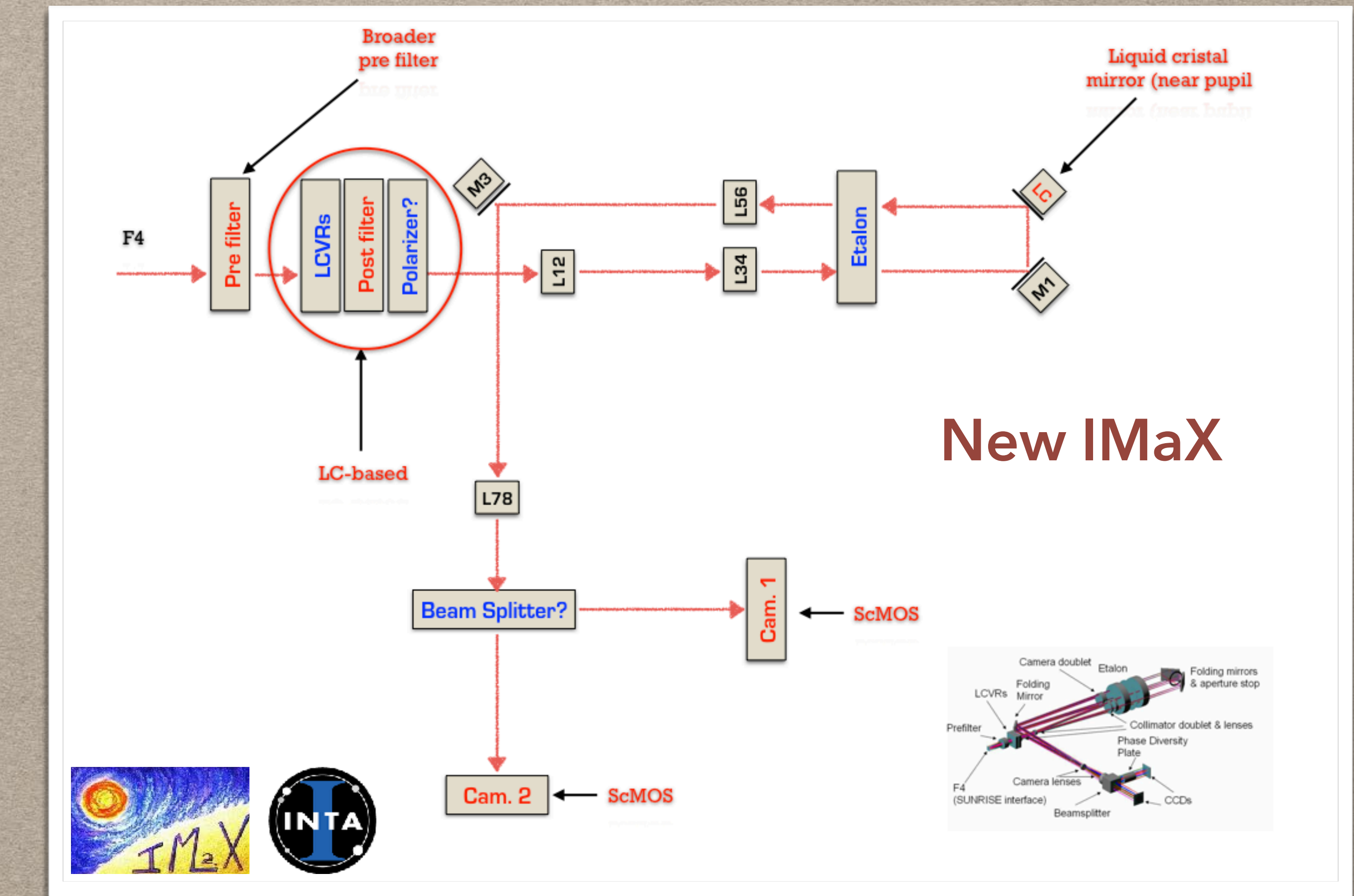
Spectral range	300 - 430 nm
Optical scheme	Littrow spectrograph with Echelle grating and off-axis aspherical mirror, slit scan unit and slit-jaw imager
Scientific target, wavelength bands	314 nm (Zeeman++) 323 nm (Scatter++) 359 nm (Scatter++) 393 nm Ca II K 397 nm Ca II H 408 nm (Zeeman++)
FOV	61" x (14.3 - 20.5) Å
sampling	0.03" x (7 - 10) mÅ/px
Cadence	5 - 20 s
Max. pol. accuracy	5×10^{-4}



IMAGING MAGNETOGRAPH EXPERIMENT (IMAX+)



Spectral range	517 - 525 nm
Optical scheme	Collimated double-pass Fabry-Pérot filtergraph
Scientific target, wavelength bands	Photosphere: Fe I 525.06 nm Fe I 525.02 nm Fe I 524.7 nm Temperature minimum: Mg I 517.3 nm
FOV	56" x 56"
Spatial & spectral sampling	0.055"/px 65 mÅ FWHM
Cadence	8 - 33 s
Max. polarimetric accuracy	< 1 x 10 ⁻³

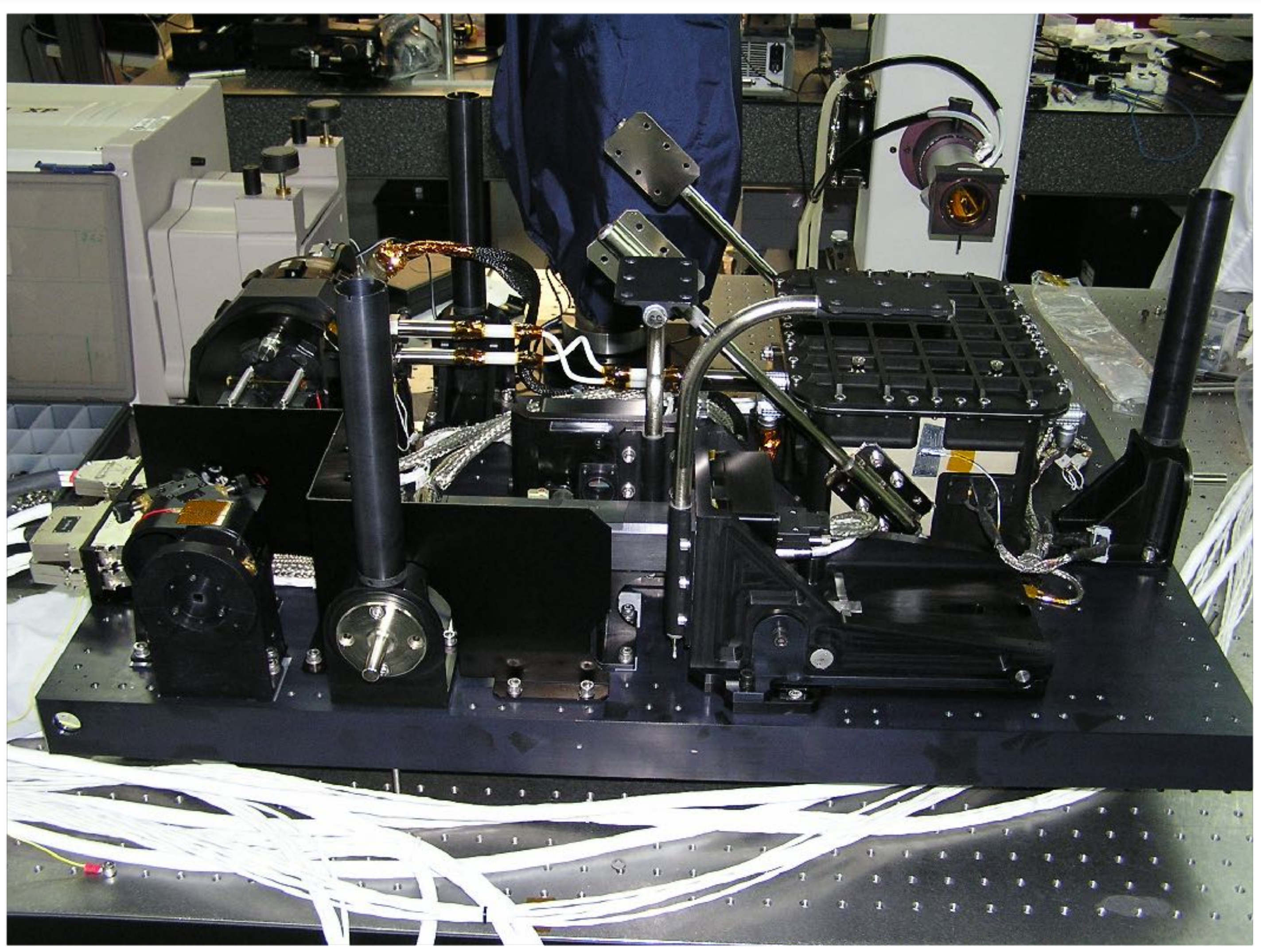


Main scientific improvement:

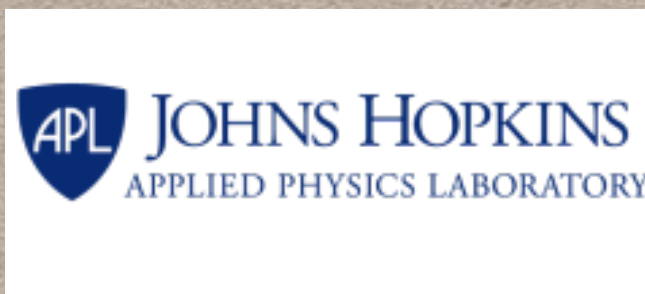
- Tuning at several wavelengths
 - Prefilter wheel
 - Tunable prefilter (Liquid Crystal Tunable Filters? Prefilter tuned by angular rotation? Others?)

Technical improvements:

- Supression of image shifts
- Improve the mechanical design to obtain a stronger stiffness
- Astigmatism suppression
- Cameras change



- Funding is approved for MPS, NAOJ and IMaX team
- MPS + NAOJ already working on hardware
- APL gondola decision pending
- Launch planned for June 2021
- Instrument system integration and test will start already one year before launch (mid 2020)



S.K. Solanki + MPS Team

Max Planck Institute for Solar System Research, Germany

P. Bernasconi + APL Team

Applied Physics Laboratory, Johns Hopkins University, USA

J.C. del Toro-Iniesta + IMaX Team

Instituto de Astrofisica de Andalucia, Spain and the IMaX consortium

Y. Katsukawa + NAOJ Team

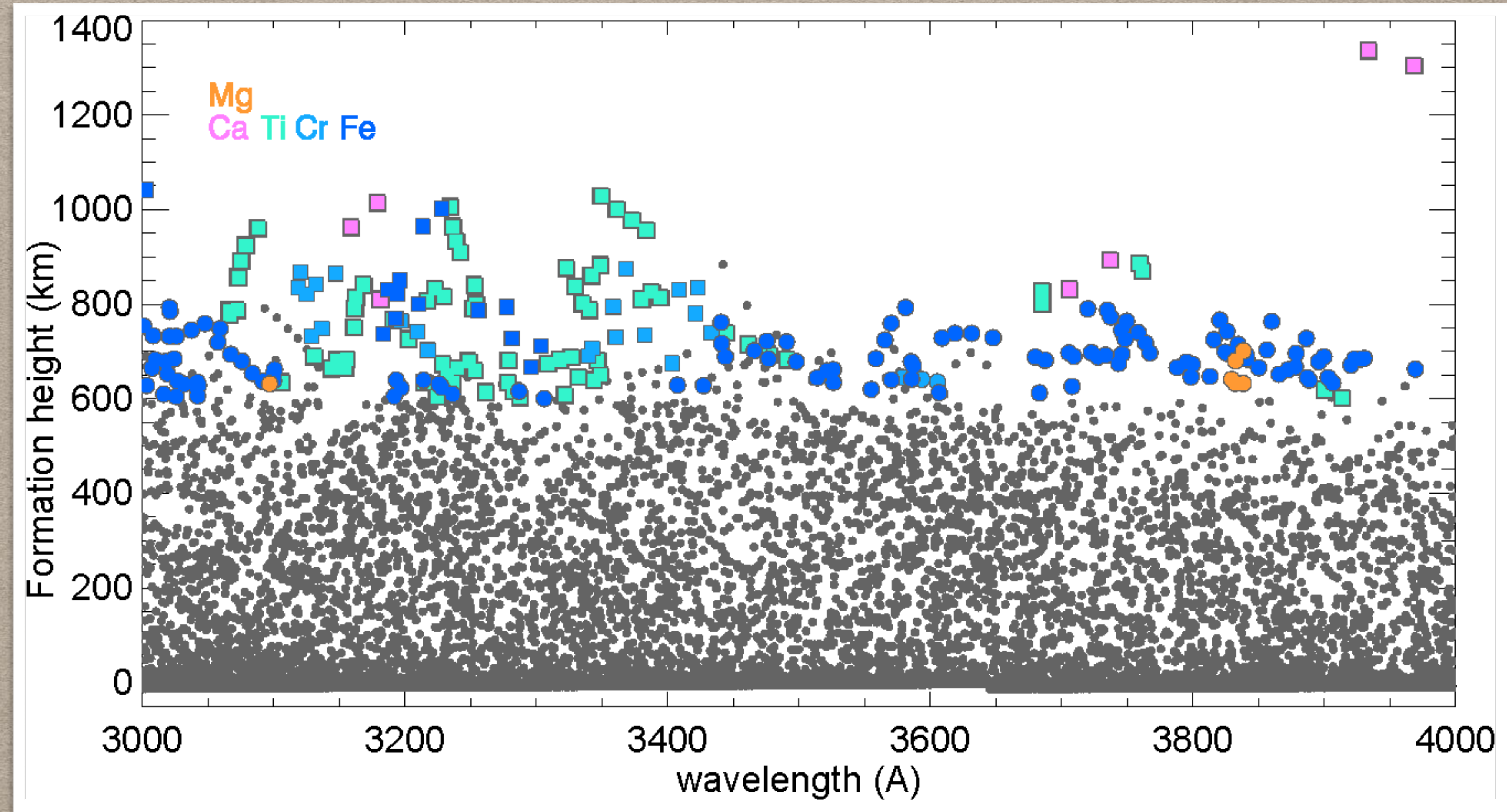
National Astronomical Observatory of Japan

T. Berkefeld + KIS Team

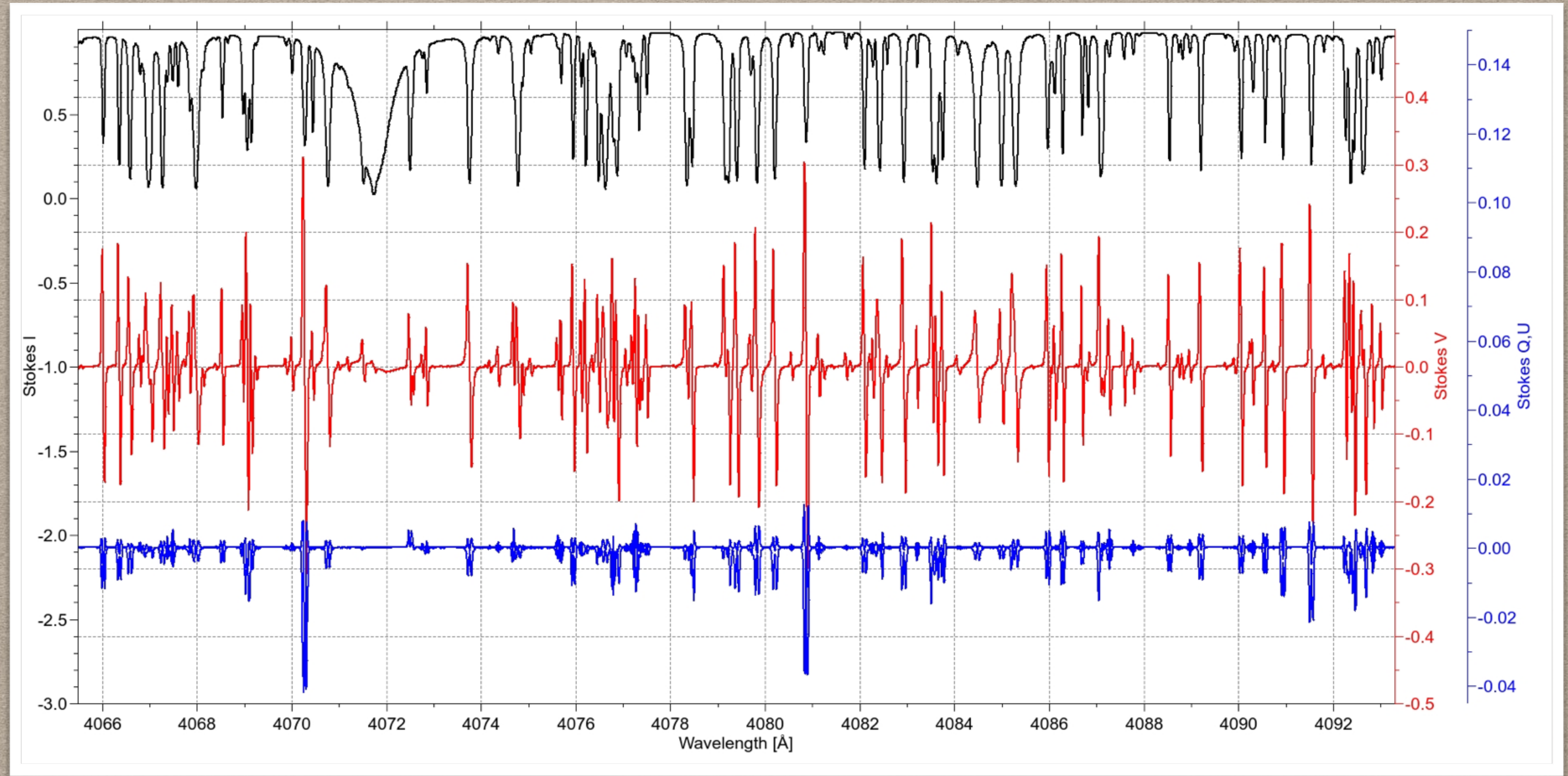
Kiepenheuer Institut für Sonnenphysik, Germany

1	Science case	1
1.1	The crucial role of the magnetic field	1
1.2	The complex magnetic field in the photosphere	1
1.3	Turbulent magnetoconvection: origin and fate of magnetic flux	2
1.4	The chromosphere	4
1.4.1	Propagation, conversion and dissipation of waves	4
1.4.2	The role of Ohmic dissipation and magnetic reconnection	6
1.4.3	Determining three-dimensional magnetic structures in the solar atmosphere	7
1.4.4	Formation of the sunspot penumbra	8
1.4.5	Photospheric and chromospheric jets	9
1.5	Exploration of the polarised solar spectrum in the UV	9

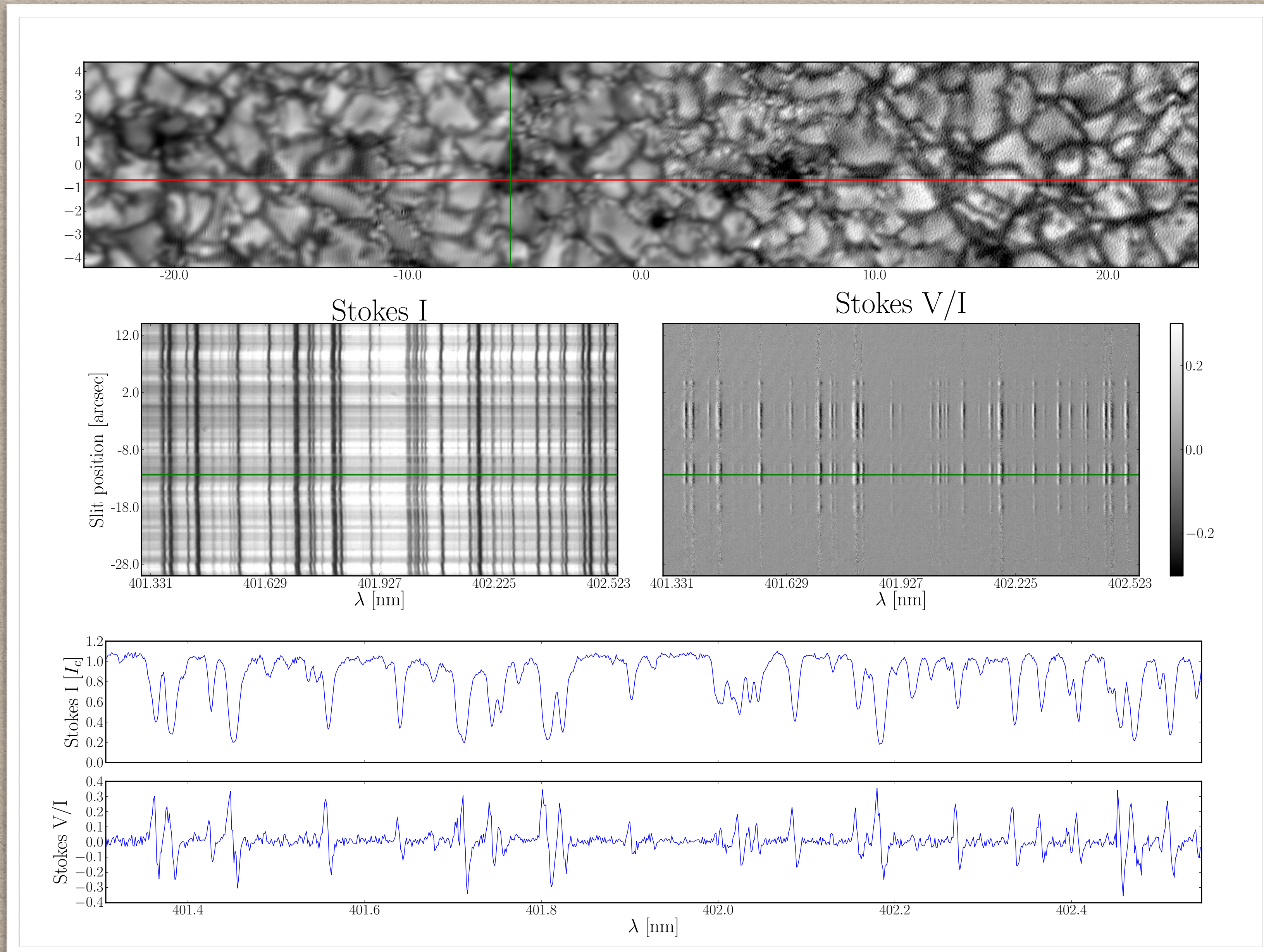
MANY-LINE ANALYSIS WITH SUNRISE III



MANY-LINE ANALYSIS WITH SUNRISE III



MANY-LINE TEST OBSERVATIONS (SST/TRIPPEL, 2016)



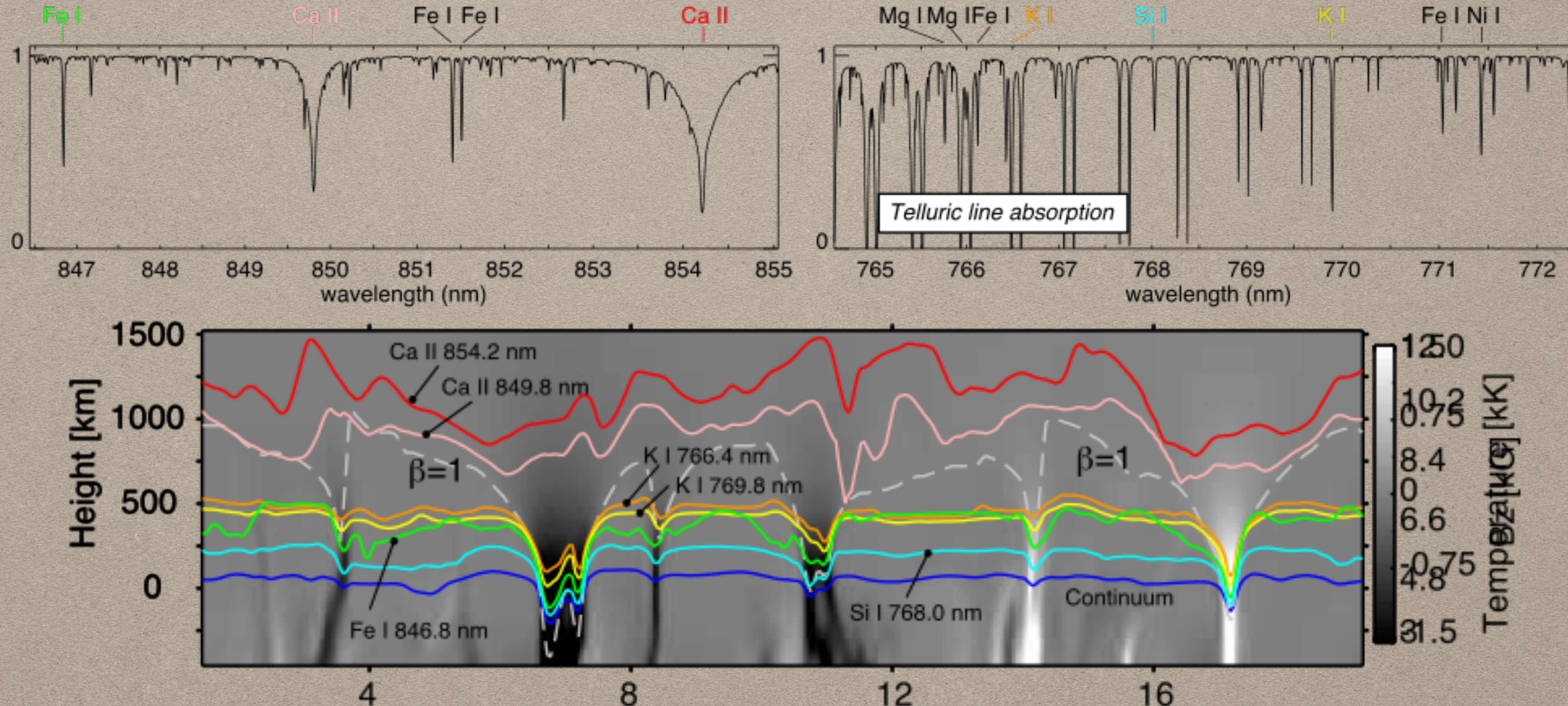
MANY-LINE ANALYSIS WITH SUNRISE III



- MHD experiments with many-line inversions show:
 - MHD cube (QS - pores)
 - Strong polarization
 - Signals available through height strat. →
 - perfect solution
 - Gain of information by possible
 - the use of many spectral
 - Synthesize spectrum
 - Spectral range contains telescopic spectral resolution lines
 - highest & seemparey of T and v_LOS measurements in

Log(τ)	σ_{314_248} [G]	σ_{408_204} [G]	σ_{630_63} [G]	σ_{630_2} [G]
-2.5	240	65	65	130
-1.5	130	84	84	120
-0.8	89	42	49	110
0	130	95	106	1000

CHROMOSPHERIC 3D OBSERVATIONS WITH SCIP



DKIST & SUNRISE III

MUTUAL BENEFIT

	DKIST	Sunrise III
spatial resolution	+++	+
height resolution	++	+++
magnetic sensitivity	+++	+++
instrumentation	+++	+
long-term stability	+	+++
atmospheric straylight	-	+++
near-UV exploration	-	+++

Boundary conditions:

- launch window:
6 week window around June 21st 2021
- launch decision: around 6am in the morning
- flight duration: 5-6 days
- DKIST FIDO setup change:
1 day
- Observing program for Sunrise to be defined in
2020
→ Sunrise III observing timeline

DKIST setup:

- imaging preferred to polarimetry (VTF + BFI (common FOV guaranteed))
- use most common FIDO setup (check all SUCs covering Sunrise science objectives)
- identify existing SUCs matching the Sunrise timeline

SUC-59 is somewhat special.
2020: write normal DKIST proposal

DKIST observations:

- Sunrise III defines pointing coordinates + scientific program will be communicated in real-time to co-observers at ground-based telescopes
- DKIST shall observe same region with the standard setup for the Sunrise III SUC (to be defined)
- as often, as long as possible.

DKIST/SUNRISE SUC: FINISH YOUR SUCs ...

